AFIT/GOR/ENS/99M-17

UNMANNED AERIAL VEHICLE MISSION LEVEL SIMULATION

THESIS

Jennifer G. Walston, Captain, USAF

AFIT/GOR/ENS/99M

Approved for public release; distribution unlimited

AFIT/GOR/ENS/99M-17

THESIS APPROVAL

NAME: Jennifer G. Walston, Captain, USAF **CLASS:** GOR-99M

THESIS TITLE: Unmanned Aerial Vehicle Mission Level Simulation

DEFENSE DATE: 8 March 1999

COMMITTEE:	**NAME/TITLE/DEPARTMENT**	**SIGNATURE**
Advisor	T. Glenn Bailey, Lieutenant Colonel, USAF Assistant Professor of Operations Research Department of Operational Sciences Air Force Institute of Technology	
Reader	Raymond R. Hill, Major, USAF Assistant Professor of Operations Research Department of Operational Sciences Air Force Institute of Technology	

The views expressed in this thesis are those of the author and do not reflect the official policy or position of the Department of Defense or the U.S. Government.

UNMANNED AERIAL VEHICLE MISSION LEVEL SIMULATION

THESIS

Presented to the Faculty of the Graduate School of Engineering
Air Force Institute of Technology
Air University
In Partial Fulfillment of the
Requirements for the Degree of
Master of Science in Operations Research

Jennifer G. Walston, A.S., B.S.
Captain, USAF

March 1999

Approved for public release; distribution unlimited

Acknowledgments

I sincerely thank all those who assisted in this endeavor. LtCol Bailey, who not only provided encouragement and support, but also pulled me out of code and back into the big picture when necessary. The UAV Battlelab for their support and for providing an interesting project in the first place. Capt Salt Bacot for his help with the weather portions of this research and SSgt Riter at the Air Force Combat Climatology Center for his outstanding support of my data request. The 11RS for answering all of my questions especially, my brother SRA David Wells for always being there when I needed an operator's opinion or a sounding board (Thanks Dave!).

I am forever grateful to my family for their unfailing support during this thesis. I thank my mother and father-in-law for their love and support; my dad for again being my rock and pillar of support when I am frazzled; and my mom for always reminding me that I can do all things through Christ, who strengthens me. I especially want to thank my husband Brad for standing by my side, always being my champion, and loving me without fail. And finally, I want to thank my Lord Jesus Christ who provided me with the ability to complete this project and the strength to see it through.

Jennifer G. Walston

Table of Contents

List of Figures

Page

Page

List of Tables

Page

Abstract

We develop an object-oriented simulation that models the surveillance and Active Suppression of Enemy Air Defense (SEAD) missions of the Unmanned Aerial Vehicle (UAV) RQ-1A Predator. The simulation, written in Java using the Silk simulation package, interfaces with a Reactive Tabu Search routing algorithm to provide optimal UAV routes. The routing algorithm is called by the simulation to account for changes in weather conditions and to provide a means of dynamically retasking the UAV. The simulation and analysis support a UAV Battlelab initiative to test the operational effects of proposed changes in Predator performance and UAV capability to perform in an Active SEAD mission. Analysis efforts examine the effect of speed, endurance, and weather susceptibility on UAV operational effectiveness and the effects of radar cross section, threat density, and threat lethality on UAV Active SEAD mission performance.

UNMANNED AERIAL VEHICLE MISSION LEVEL SIMULATION

I. Introduction

As the employment of unmanned aerial vehicles (UAVs) for military operations increases, so will demand for new and innovative tactics and techniques involving their use. However, implementing such techniques requires testing. As one of six Battlelabs set up by the Air Force to test the feasibility and effectiveness of new ideas in a timely manner, the UAV Battlelab (UAVB) has responsibility for testing UAV system initiatives. Since physical testing is extremely costly, the UAVB requires a mission-level simulation tool to provide additional data for evaluation. Therefore, this research provides a prototype simulation model and initial analysis for the Predator UAV program. A simulation will not always prove a certain initiative both feasible and operationally acceptable; however, it does provide a mechanism to filter out unusable initiatives. Therefore, we concentrate on helping the UAVB focus its time and resources on those initiatives that warrant further investigation. We demonstrate this approach by analyzing a Kenney Battlelab Initiative (KBI), Active SEAD, and an additional effort to improve UAV Performance.

II.1. Introduction

As the employment of unmanned aerial vehicles (UAVs) for military operations increases, so will demand for new and innovative tactic and techniques involving their use. Currently, UAVs are primarily used for reconnaissance and surveillance missions; however, in the near future UAVs may assume traditional manned aircraft missions. For example, missions traditionally performed by manned crews, like the Suppression of Enemy Air Defenses (SEAD), are being considered for assignment to UAVs (Breshears, 1996: 315). This idea is not new--the first instance of a UAV used in a lethal strike mission occurred over Europe in World War I (Breshears, 1996: 315). Indeed, with the advent of the technological advances since that first UAV and the desire to protect human pilots, the role of UAVs in historically manned-only missions will most likely expand in the future.

Implementing such techniques requires testing. As one of six Battlelabs set up by the Air Force to test the feasibility and effectiveness of new ideas in a timely manner, responsibility for testing UAV system initiatives lies with the UAV Battlelab (UAVB). Since physical testing is extremely costly, the UAVB requires a mission-level simulation tool to provide additional data for evaluation. One such tool, a Teledyne Brown Engineering model, Extended Air Defense Simulation (EADSIM), has been used to some extent for this purpose. However, because EADSIM was designed for the SEAD mission and not specifically for UAVs, a customized model for the UAV can provide key insights into the results of the initiatives on the desired performance parameters of the UAVs. Therefore, this research provides a prototype simulation model and initial analysis for the

Predator UAV program. A simulation will not always prove a certain initiative both feasible and operationally acceptable; however, it does provide a mechanism to filter out unusable initiatives. Therefore, we concentrate on helping the UAVB focus its time and resources on those initiatives that warrant further investigation.

We demonstrate this approach by analyzing a Kenney Battlelab Initiative (KBI), Active SEAD, and an additional effort to improve UAV Performance:

> *Active SEAD.* We investigate the ability of a UAV to perform an active SEAD mission. Specifically, this simulation examines input parameters such as UAV Radar Cross Section and potential threats to verify UAVs ability to decoy, detect, identify, jam, and target threat systems either independently or as part of a package in a realistic active SEAD environment. Potential measures of effectiveness (MOEs) include number of UAVs destroyed, number of UAVs engaged, and percentage of mission accomplished (USAF ACC, 1998a: Sect. 1.1 to 2.2).
>
> *Aircraft Performance.* We determine the operational effect of Predator performance parameter changes. This analysis applies directly to the aircraft performance improvement effort currently being studied by the Department of Aeronautics at the United States Air Force Academy (USAFA) in cooperation with the UAVB. USAFA intends to use our simulation to determine the operational effects of changes to the speed capability of the Predator using target detection as the measure of effectiveness (Brandt, 1998). We provide input and output variables applicable to their work and an initial analysis and results.

This research fits into a framework depicted in Figure 1. Specifically, we provide a discrete event simulation model of the UAV flight environment that connects to a routing algorithm that provides near-optimal vehicle routing information. This capability provides a real-time optimization link into the simulation to facilitate route changes to the UAV mission, and allows the simulation to model dynamic re-tasking (a necessary function for the Active SEAD Battlelab initiative concept of operation). The Graphical User Interface (GUI) facilitates model input and output.

The complete simulation package interacts in a tri-modal framework in the following manner:

> *Graphical User Interface.* The GUI provides the input data to the simulation from the keyboard and from data files and provides output data storage and report generation capabilities. The GUI will be linked to the simulation in follow-on research.
>
> *Optimization Routine.* The Optimization Routine provides the simulation with UAV routes at any time in the scenario. The routes are calculated using Reactive Tabu Search to solve the Multiple Traveling Salesman Problem with Time Windows (mTSPTW) (O'Rourke, 1999). The provided routes allow the simulation to emulate the decisions made by the UAV sensor operators (thereby modeling the dynamic rerouting capability). By using an optimization tool to mimic the decision process, we reduce the chance of confounding the simulation output by uncontrollable factors. The routing algorithm provides a logical control for the routing decision.

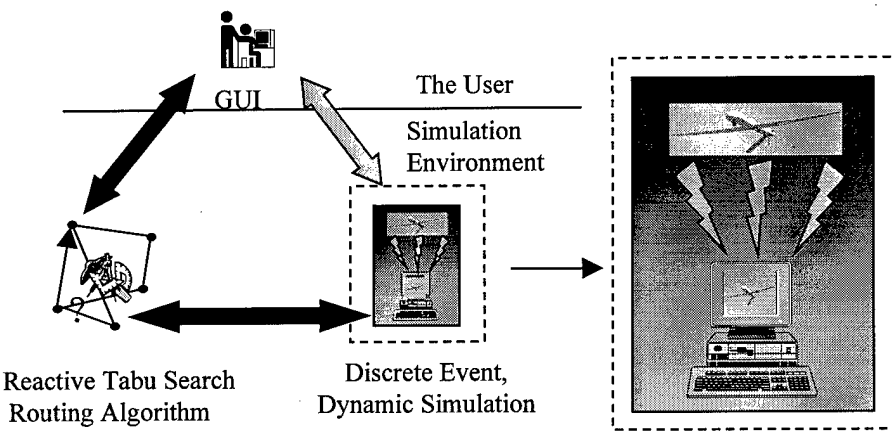

Figure 1: Framework for the UAV Model

We present our results in the following manner. Section 2 discusses the background of the study including related research. Section 3 describes the simulation model including verification and validation efforts. Section 4 presents the experimental design, case studies, and results. Section 5 relates our observations and conclusions.

II.2. Background and Related Research

EADSIM has been used to a limited extent by the UAV Battlelab to test new initiatives in communications (Theisen, 1998). Army Materiel Systems Analysis Activity developed a PC-based model that compares UAV survivability with both the Predator Synthetic Aperture Radar and Hunter Forward-looking Infrared systems during UAV acquisition (USA AMC). The Institute for Defense Analyses, in support of Director, Operational Test and Evaluation (DOT&E) has developed an event-step Monte Carlo simulation to assist Predator analysis, particularly Effective Time on Station as affected by suitability factors like maintenance resources allocated. This model has recently been extended for incorporation into the Military Aircraft Sustainability Simulation (MASS) program (Stoneman, 1998: xiii).

Sisson (1997) employs reactive tabu search for deterministic vehicle routing problems of UAVs. His approach includes wind effects and adds risk avoidance and expected coverage into the objective function of the routing algorithm to account for UAV attrition. A Monte-Carlo simulation then checks generated routes to estimate the expected number of targets covered. His work basically provides only a snapshot look at the UAV environment and its effects on the routing.

Ryan et al. (1999) extend Sisson's research by incorporating weather effects and probability of survival as random inputs into a discrete-event simulation that calls the routing algorithm. Additionally, their research identifies robust routes, routes less

sensitive to weather and threat changes, and provides an object-oriented library that more easily facilitates the study of UAV routing problems.

This research expands on the previous work of Sisson and Ryan by providing a *dynamic* environment in that changes affect the UAV *enroute*. With the length of the UAV mission (as long as 24 to 42 hours), time-dependent parameters cannot be adequately represented statically in a Monte-Carlo simulation. Therefore, it is imperative to model these parameters, like weather, dynamically. However, research to date has been static in nature. This research provides a dynamic model to analyze UAV missions.

II.3. Model Development

II.3.1 Simulation Model

The simulation is discrete event and dynamic (*i.e.* time-dependent), written in the Java programming language using the SILK simulation package. The object-oriented nature of Java facilitates the creation of multiple UAVs, Ground Control Stations (GCSs), all required entities and resources, and the assignment of individual attributes to the created objects. The major operational factors we specifically capture include weather (rain, ice and winds aloft), dynamic rerouting, and susceptibility to enemy defenses. (Reliability of the platform, GCS, and satellite are relatively high and therefore are not specifically modeled in this version of the simulation.) These major parameters are modeled stochastically; for example, weather is represented as a probability density

function of several representative cases. Every case contains a 24-hour weather trace to be run by the simulation. Each specific replication is a random draw from these representative cases. Specific Java classes for the simulation are shown below in Figure 2.

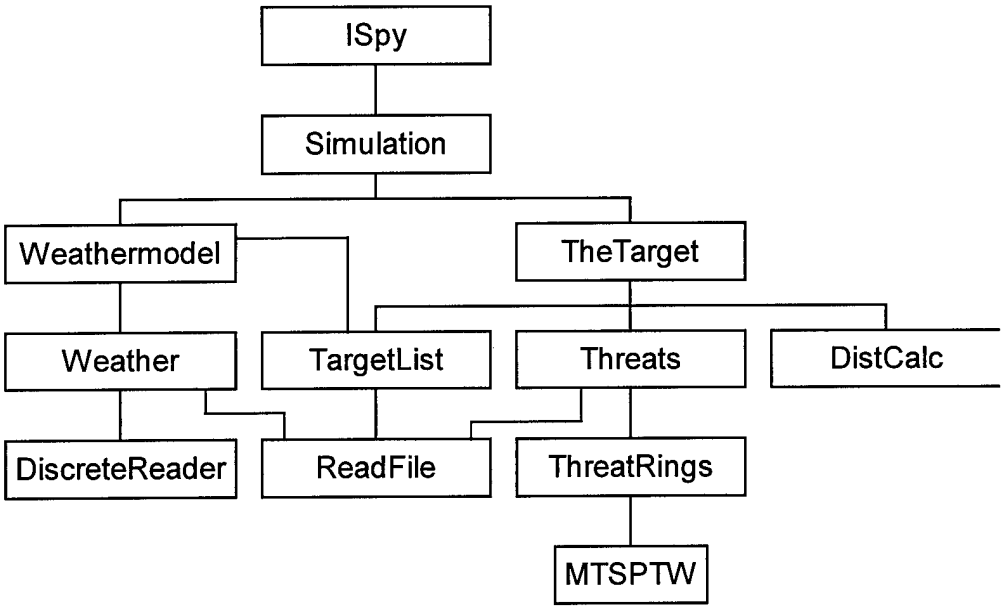

Figure 2: Java Class Interaction for the Simulation

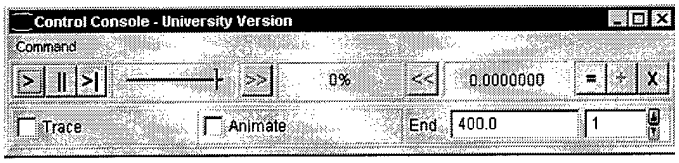

Figure3: Silk Control Console

The Java Classes function and interact as follows:

ISpy. This class creates an application where the simulation package Silk runs. It creates a simulation control console as shown in Figure 3.

Simulation. This class begins the simulation when the start button on the simulation tool bar is clicked. It creates the first instances of the classes *WeatherModel* and *TheTarget*. After the first instance, these two classes self-replicate. A single additional instance of *WeatherModel* is created to read in the weather data and to draw a weather trace for each replication. A single instance of *Threats* is created to read in the threat data.

WeatherModel. This class calls the *Weather* class every 60 time units to update the weather for the simulation by reading the next weather in the weather trace. It also contains methods to read in the weather data files and distribution, and to randomly draw a weather file by calling methods from the *DiscreteReader* class.

Weather. This class contains the weather files used to update the weather. It calls methods from the *ReadFile* class.

TheTarget. This class calls the *TargetList* class to obtain the location of the next target, then calls the *DistCalc* class to determine the time to reach that target. If the time to the next target and then home base does not exceed the UAV endurance, it schedules the next target. Otherwise, it schedules return to home base. However, before scheduling either of these arrivals it calls methods from *Threats* to determine if the UAV will be destroyed before the arrival can occur. If so, the arrival is not scheduled and the replication terminates upon UAV destruction.

TargetList. This class contains the target list for the UAV. It calls methods from the *ReadFile* class to read in the targets from a data file. It also contains the interface to the Reactive Tabu Search routing algorithm by calling the methods from the class *MTSPTW*. By calling *MTSPTW* for a new route, this class updates the target list every 120 time units.

Threats. This class contains the threat list. It calls methods from the *ReadFile* class to read in the threats from a data file. It provides methods to determine UAV destruction based on lethality and a call to the range determination method in the class *ThreatRings*.

DistCalc. This class contains the methods to calculate the time to the next target based on UAV speed and wind information.

ReadFile. This class contains the methods to read variables in from a data file.

ThreatRings. This class provides the methods to determine if a UAV is in range of any of the threats.

DiscreteReader. This class provides methods to chose a random variate from a given distribution.

MTSPTW. This class is the main interface to the Reactive Tabu Search routing algorithm. The method Route is called by *TargetList*, while the remainder of the routing algorithm is treated as a black box.

As stated above, we model the weather as trace-driven replications using a series of representative 24-hour weather observations as weather inputs to the simulation. These representative cases are randomly drawn by the simulation based on a distribution of the weather patterns in the scenario region of Bosnia-Herzegovina. Seven weather sites are used to divide the region as shown in Figure 5. The distribution is determined

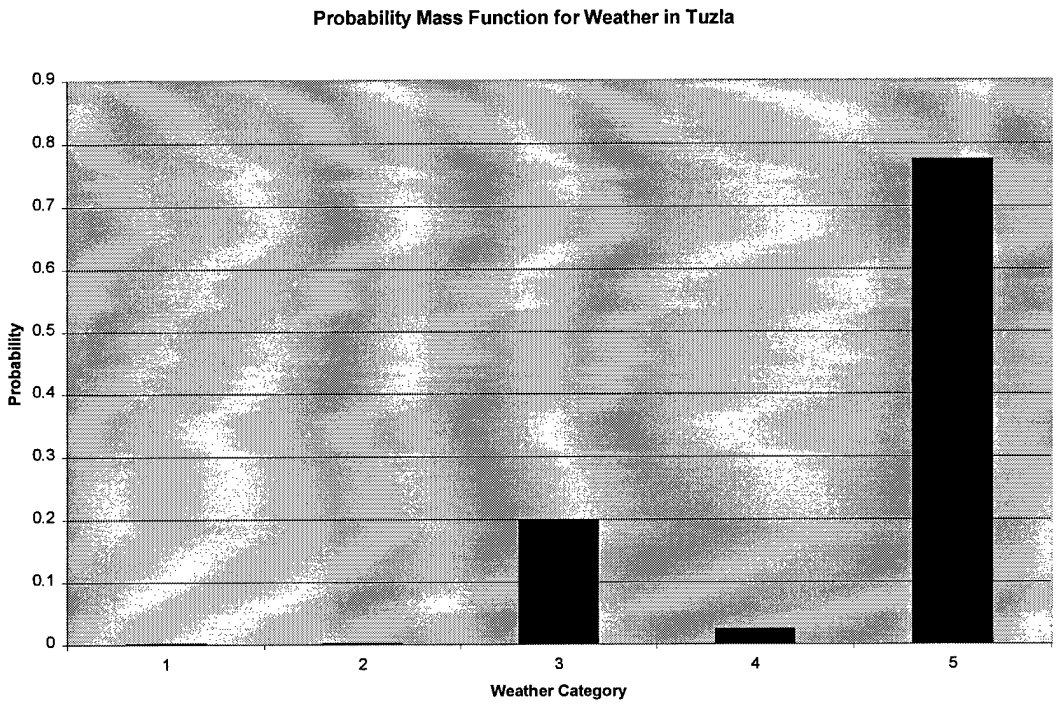

Figure 4: Example Weather Probability Distribution for Tuzla, Bosnia-Herzegovina

using historical weather information for a 20- to 25-year period (depending on the weather site) as provided by the Air Force Combat Climatology Center (AFCCC). (Each case has one associated weather file. Data used to determine the probability function is

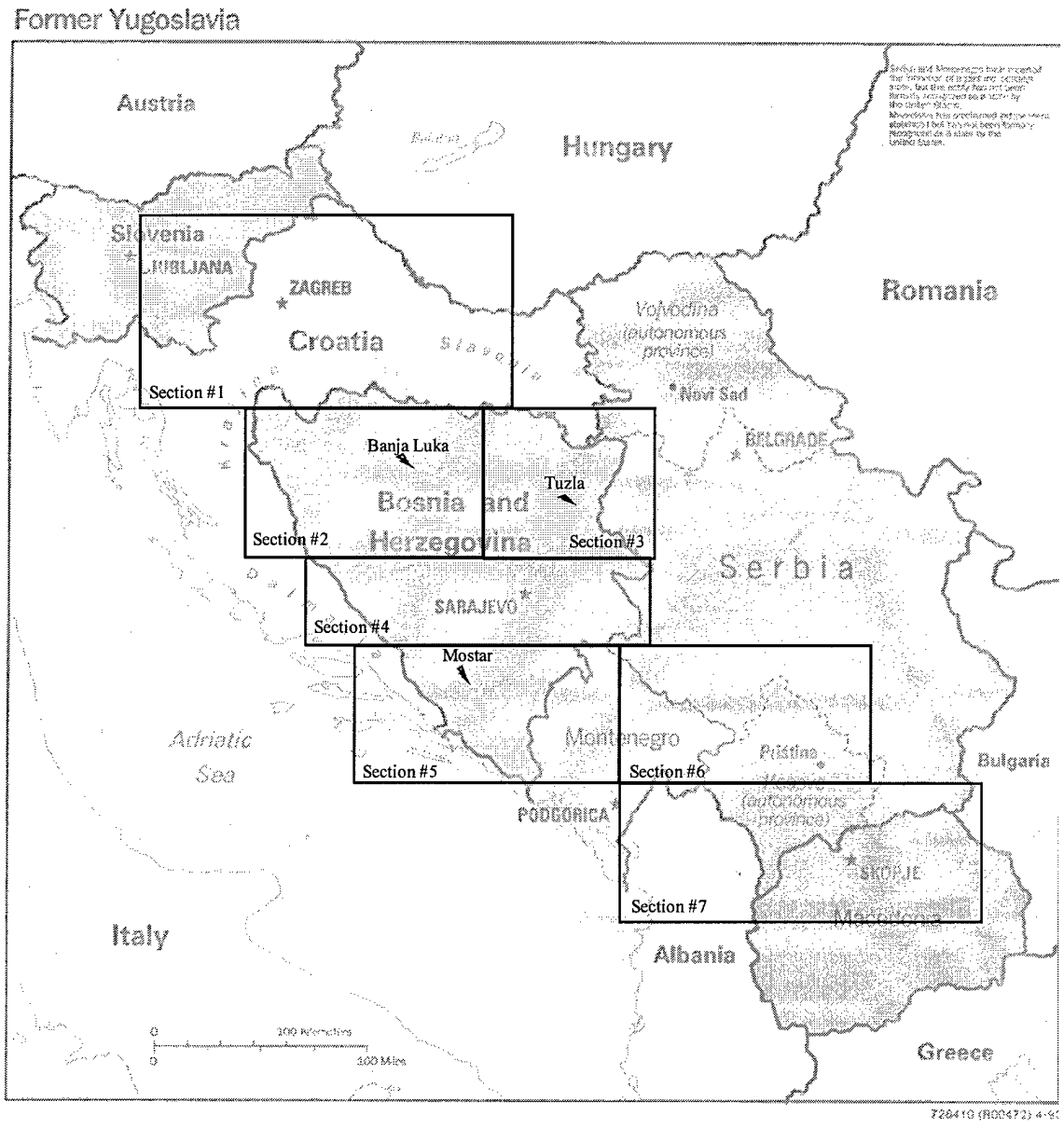

Figure 5: Sections of Weather Observations in Bosnia

shown in Appendix C.) For example, with five different representative weather files for each weather site (1-Crosswinds, 2-High Winds, 3-Ceiling/Visibility, 4-Rain, 5-Fair Weather) and a probability of occurrence associated with each, the simulation randomly draws a weather condition. The data for this condition is then used for that replication. A sample distribution is shown in Figure 4. We model wind direction separately with a probability distribution derived from historical prevailing wind information for the entire region. Wind direction is updated via a random draw from this distribution at every weather update.

A method in the class *ThreatRings* determines if a UAV passes within range of a threat. Assuming the threat range is equal in all directions (*i.e,* no obstructions), we represent the area of danger as a circle, *i.e.* threatened. The minimum distance from a line to a point is given by (Anton, 1988: 46, 818-819)

$$D = \frac{|aX_0 + bY_0 + c|}{\sqrt{a^2 + b^2}}$$

where X and Y are illustrated in Figure 6 and

$$(Y - Y_1) = \left[\frac{Y_2 - Y_1}{X_2 - X_1}\right](X - X_1) \quad \Rightarrow \quad \begin{aligned} a &= (Y_2 - Y_1) \\ b &= (X_1 - X_2) \\ c &= (Y_1 - Y_2)X_1 + (X_2 - X_1)Y_1 \end{aligned}.$$

If the distance between the path of the UAV and the threat is less than the range (or radius), the UAV is in the circle.

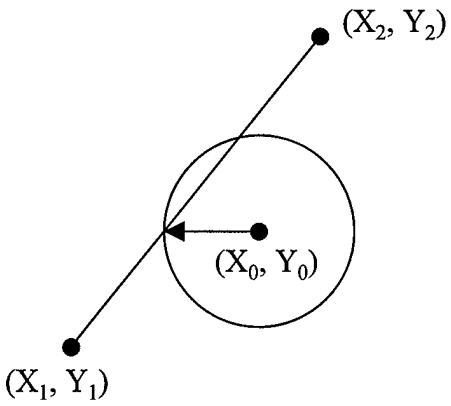

Figure 6: UAV Path Through Threat Ring

II.3.2 Verification

We verify and validate (V&V) the model according to the guidelines for developing new models shown in Figure 7 using trivial case and extreme value data,

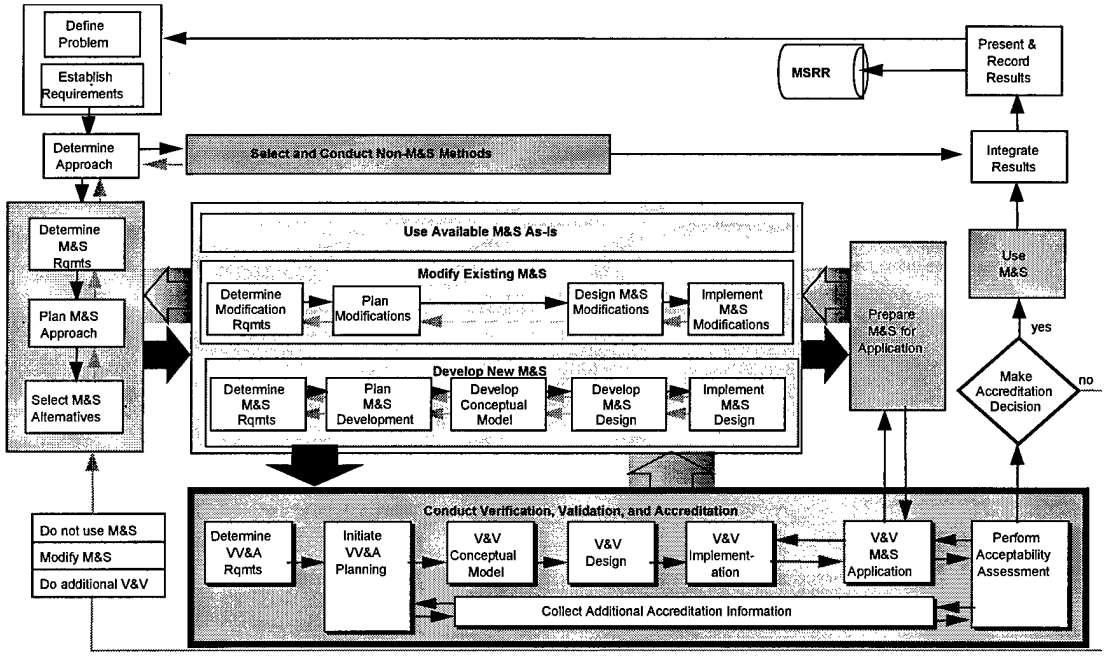

Figure 7: The Generic VV&A Process in the M&S Lifecycle (DoD, 1996: 3-20)

respectively. Using simple data and line-by-line analysis, we verify that the simulation algorithms and logic are correct. Specific techniques include:

> *Execution Tracing.* This verification technique reveals errors by analyzing the step-by-step execution of a simulation (DoD, 1996: 4-20).

We trace the simulation execution both on the screen and to a series of files during verification runs. Additionally, on-screen traces were used extensively during model development. Verification runs were accomplished for cases where a UAV would be destroyed and those where it would reach endurance limitations. In both cases, the simulation traces were correct.

> *User Interface Testing.* This method detects errors in model representation resulting from user-model interface errors or invalid interface assumptions (DoD, 1996: 4-24).

We verified the user inputs (reading of data files) to the weather classes and the threat classes using on-screen messages when the simulation was developed. We verified the user inputs of the target classes by writing out the target list to a data file and comparing it to the input.

> *Model Interface Testing.* The technique detects errors in model representation resulting from submodel-to-submodel or federate-to-federate interface errors or invalid interface assumptions (DoD, 1996: 4-23).

We verified the weather class interfaces using on-screen messages when the simulation was developed. We checked the interface to the routing algorithm using on-screen reports and outputs to data files to verify the returned sequence of the target list and to ensure the entrance and exit corridor was used.

II.3.3 Validation

Validation compares operational data to model output. Hypothesis testing then checks that the two are statistically similar. Specific techniques include:

> *Extreme Input Testing.* This validation method runs the model or simulation with minimum values, maximum values, or an arbitrary mixture of minimum and maximum values for the model input variables (DoD, 1996: 4-28).

Using speed and endurance as inputs to the extreme input testing, we discovered the following. If the UAV airspeed is less than the component of wind in that direction, the simulation calculates a time to next target as infinite and the simulation terminates. This is not a problem in our case studies, as the speed regime is significantly higher than the minimum value. However, the possibility of a UAV being trapped by high winds in fact exists and is a concern of the UAV community. If the simulation were then to be used in high wind conditions, the time/distance calculations would need to be altered accordingly. When combinations of low speed and low endurance cause the simulation to end before reaching the first target past the entrance corridor, it is difficult to determine how many way points are reached in the corridor, *i.e.* how far through the corridor the UAV proceeds before returning to base. It is not necessary for our measures, but could be a valuable improvement in the future.

II.4. Scenarios and Experimental Design

II.4.1 Experimental Design Review

We selected a Central Composite Design (CCD) for this study to fit second-order response surfaces (Myers, 1995: 55). For k input factors, the CCD uses two-level factorial (2^k) points in combination with $2k$ axial points and center points. The factorial points contribute to the estimation of first order interactions between controls, the axial points contribute to the estimation of quadratic terms, and the center points provide an estimate of pure error and contribute to the estimation of quadratic terms (Myers, 1995: 298). Rotatability is a desirable property in an experimental design since it ensures that

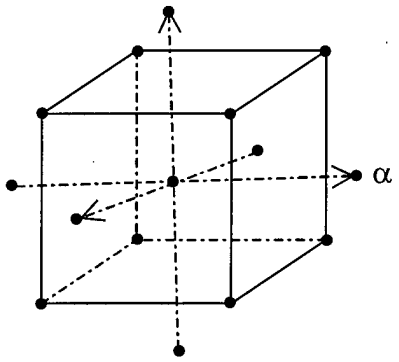

Figure 8: Central Composite Design for k = 3 and $\alpha = \sqrt{3}$ (Myers, 1995: 299)

the prediction variance is constant for any given distance from the design center, *i.e.* it is constant on spheres. (Myers, 1995: 306-312) The location of the design points in the CCD provide symmetry in the design and furnish the property that the odd design moments through order four are zero (the first of two necessary and sufficient conditions

for a rotatability). The location of the axial points at $\alpha = \sqrt[4]{2^k}$ provide the other necessary and sufficient condition for rotatablity.

Simulation replications provide input for development of a second-order model of Measures of Effectiveness (MOEs) versus changes in input parameters using a CCD. MOEs (output variables) include number of sorties, range, and coverage, and number of UAVs destroyed. The scenarios use correlated sampling to distinguish actual effects from random noise, and to reduce the variance of the estimated difference of the performance measures (Banks et al. 1996: 475). We use regression to determine the effects of the performance parameters on operations (Myers, 1995: 84), and hypothesis testing and ANOVA to determine if there is a statistically significant change in the operational effect.

II.4.2 Scenario 1--Active SEAD

As previously stated, we investigate the ability of a UAV to perform an active SEAD mission. Input parameters and MOEs are shown in Table 1 and the design matrix is shown in Table 2. We assume UAV airspeed is 65 knots, UAV endurance is 10 hours, and the probability of enemy engagement is 85%.

Table 1: Active SEAD Parameters and MOEs (USAF ACC, 1998a: Sect. 1.1 to 2.2)

Input Parameters	Measures of Effectiveness
UAV Radar Cross Section	Number of UAVs Destroyed
Potential Threats	Number of UAVs Engaged
Lethality of Threats (Probability of Kill)	Percentage of Mission Accomplished

Table 2: Active SEAD Design Matrix

	Coded Point			Uncoded Point		
	Probability of Detection	Number of Threats	Threat PK	Probability of Detection	Number of Threats	Threat PK
Corner Points	-1	-1	-1	0.25	6	0.01
	-1	-1	1	0.25	6	0.05
	-1	1	-1	0.25	15	0.01
	-1	1	1	0.25	15	0.05
	1	-1	-1	0.75	6	0.01
	1	-1	1	0.75	6	0.05
	1	1	-1	0.75	15	0.01
	1	1	1	0.75	15	0.05
Axial Points	-1.68	0	0	0.1	11	0.03
	0	-1.68	0	0.5	3	0.03
	0	0	-1.68	0.5	11	0
	1.68	0	0	0.9	11	0.03
	0	1.68	0	0.5	18	0.03
	0	0	1.68	0.5	11	0.06
Center Points	0	0	0	0.5	10	0.03
	0	0	0	0.5	10	0.03
	0	0	0	0.5	10	0.03

Number of UAVs Destroyed. The 90% confidence intervals for the average number of UAVs destroyed at each design point is shown in Figure 9. The non-overlapping intervals at several design points indicate that there is a statistically significant difference in the MOE between those points (Wackerly et al., 1996). However, because multiple comparisons are to be made, a Tukey-Kramer multiple comparison is performed. This test is chosen because it is appropriate for studies of all pair-wise comparisons and is useful when the family of inferences of interest is not known in advance, *i.e.* data snooping (Neter et al., 1996: 738). The results (Figure 10) are interpreted as follows. Circles for means that are significantly different either do not intersect or intersect slightly so that the outside angle of intersection is less than 90

degrees. If the circles intersect by an angle of more than 90 degrees, or if they are nested, the means are not significantly different (Sall et al.,1996: 158-159.). Therefore, even with multiple comparisons, we see statistically different responses between design points.

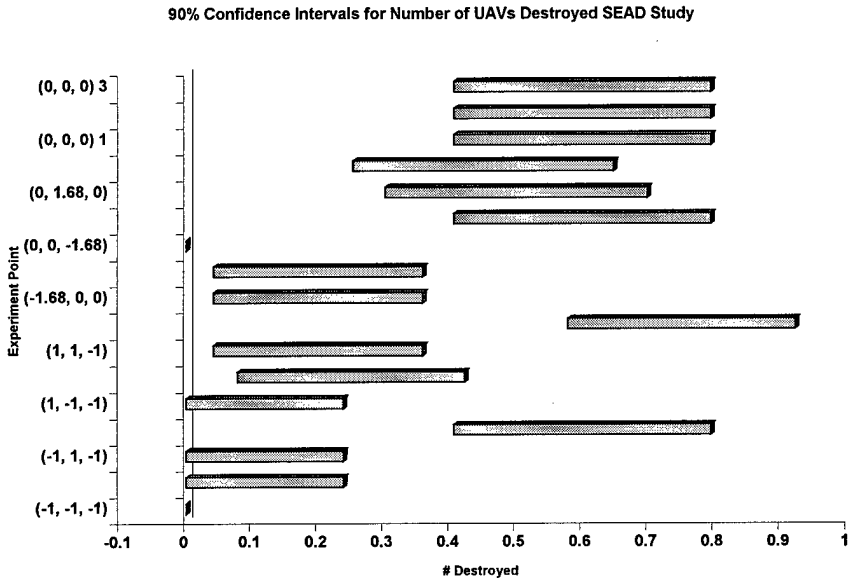

Figure 9: 90% Confidence Intervals for Number of UAVs Destroyed (SEAD Study)

To better understand the reaction of the MOE, we construct a response surface of the number of UAVs destroyed using SAS/JMP. The R^2 for this model is 0.53, indicating that we are not explaining a significant portion of the response (Figure 11). Additionally, the residuals of the model do not meet the normality assumptions of regression. We feel that this is due to high variability in the response, *i.e.* values are binary. Also, because only one kill is possible for each replication, the average number of UAVs destroyed at each design point is a more appropriate value to study. Therefore, we constructed an additional response surface for the average number of UAVs destroyed (Figure 12). R^2

for this model is 0.997 and we fail to reject the assumption of normality in a Shapiro-Wilks test for normality.

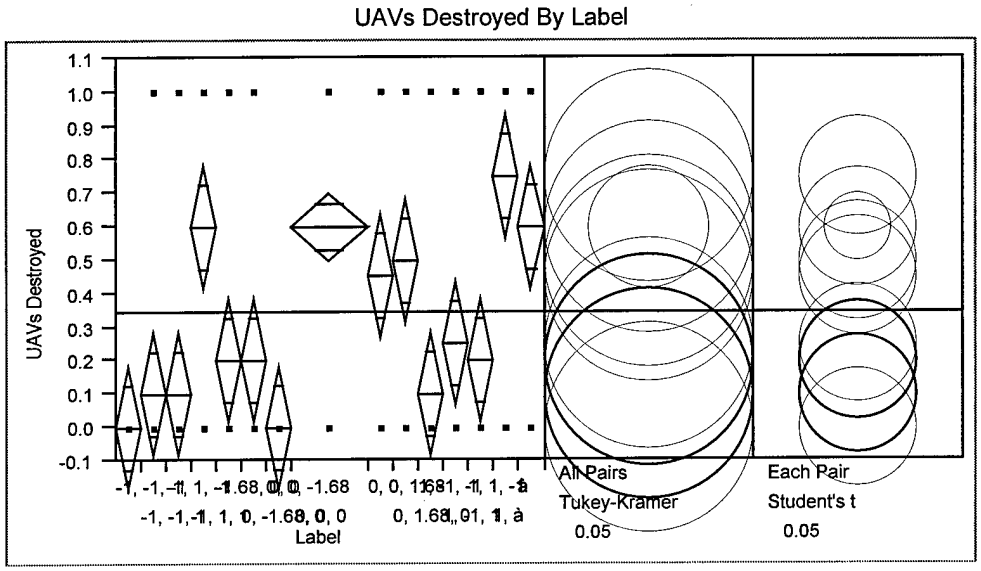

Figure 10: Tukey-Kramer Multiple Comparison Procedure for Number of UAVs Destroyed (SEAD)

Screening Fit
UAVs Destroyed
Summary of Fit

RSquare	0.527153
RSquare Adj	0.512781
Root Mean Square Error	0.3321
Mean of Response	0.344118
Observations (or Sum Wgts)	340

Analysis of Variance

Source	DF	Sum of Squares	Mean Square	F Ratio
Model	10	40.452798	4.04528	36.6785
Error	329	36.285438	0.11029	Prob>F
C Total	339	76.738235		<.0001

Figure 11: Response Model for Number of UAVs Destroyed (SEAD Study)

Screening Fit
UAV Destroyed
Summary of Fit

RSquare	0.997471
RSquare Adj	0.989882
Root Mean Square Error	0.025327
Mean of Response	0.344118
Observations (or Sum Wgts)	17

Analysis of Variance

Source	DF	Sum of Squares	Mean Square	F Ratio
Model	12	1.0118459	0.084320	131.4496
Error	4	0.0025659	0.000641	Prob>F
C Total	16	1.0144118		0.0001

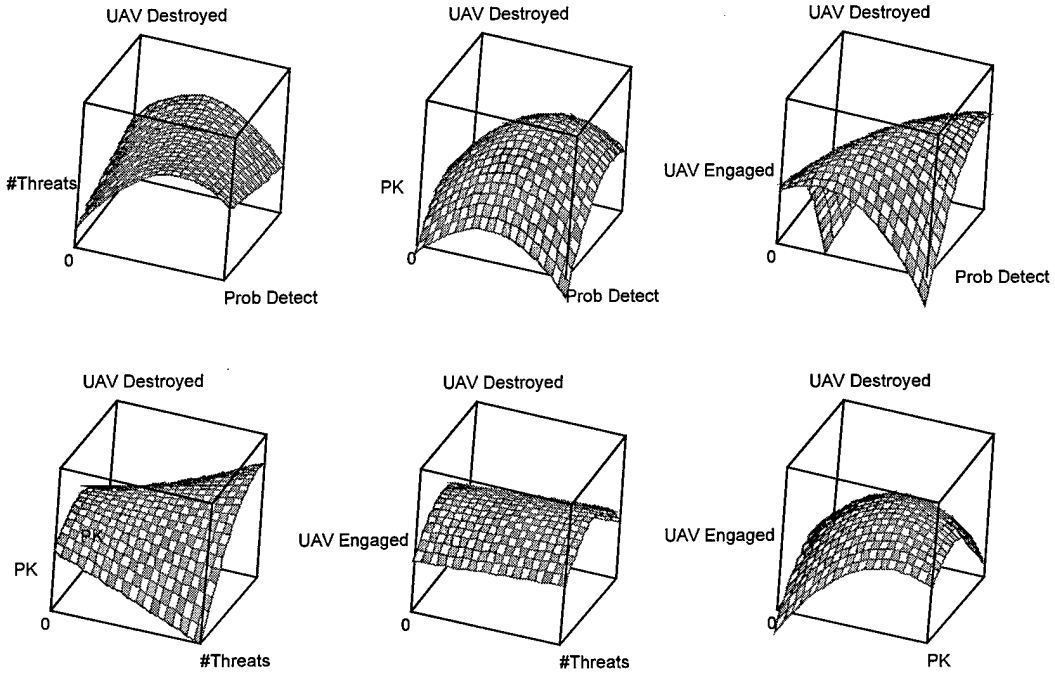

Figure 12: Response Surface for Average Number of UAVs Destroyed (SEAD Study)

As expected, we see that the number of UAVs destroyed tends to increase as the three control variables increase. However, due to interactions between controls it is not a linear function, nor does the increase continue throughout the entire region. Additionally, the number of UAVs destroyed increases with number of engagements, but again this is not a linear relationship. The interaction between the number of engagements and both

number and lethality of threats indicate that there is a point of diminishing returns, *i.e.* where the rate of increased UAV destruction begins to decline. This phenomenon, though appealing, is misleading. As threat quantity and lethality increase, the number of UAVs destroyed increases. When a UAV is destroyed, the replication terminates, thereby preventing any further engagements. Therefore, fewer UAVs reach high levels of engagements before destruction. Further investigation into multiple UAVs would provide more information.

Number of UAVs Engaged. The 90% confidence intervals for the number of times the UAV is engaged per mission is shown in Figure 13 and the Tukey-Kramer results are shown in Figure 14. Again, we find that there is a statistical difference in the average response at the design points. The constructed response surface is shown in

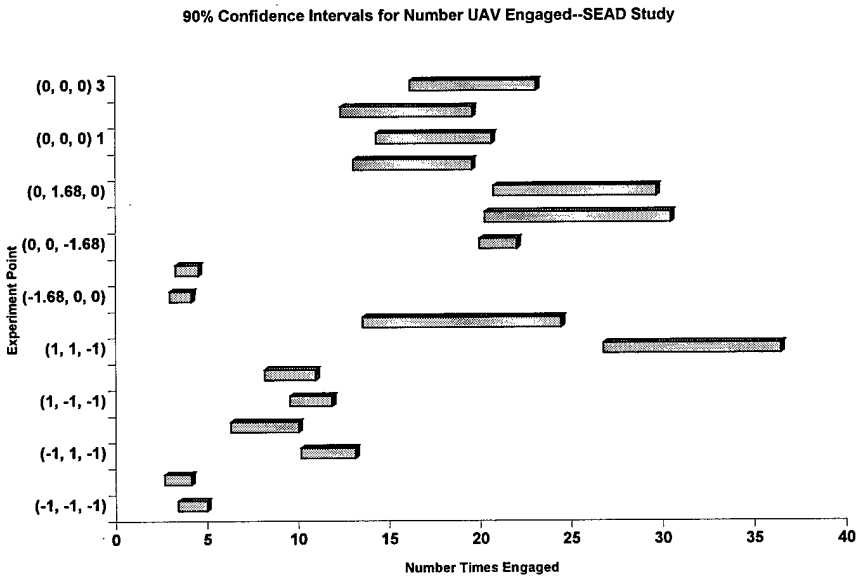

Figure 13: 90% Confidence Intervals for Number of Times UAV Engaged (SEAD Study)

Figure 15. The R^2 for this model is 0.72, but again the residuals are not normal. By again regressing on the average values of the response, we construct the response surface shown in Figure 16. The R^2 is .989 and the model meets the normality assumptions.

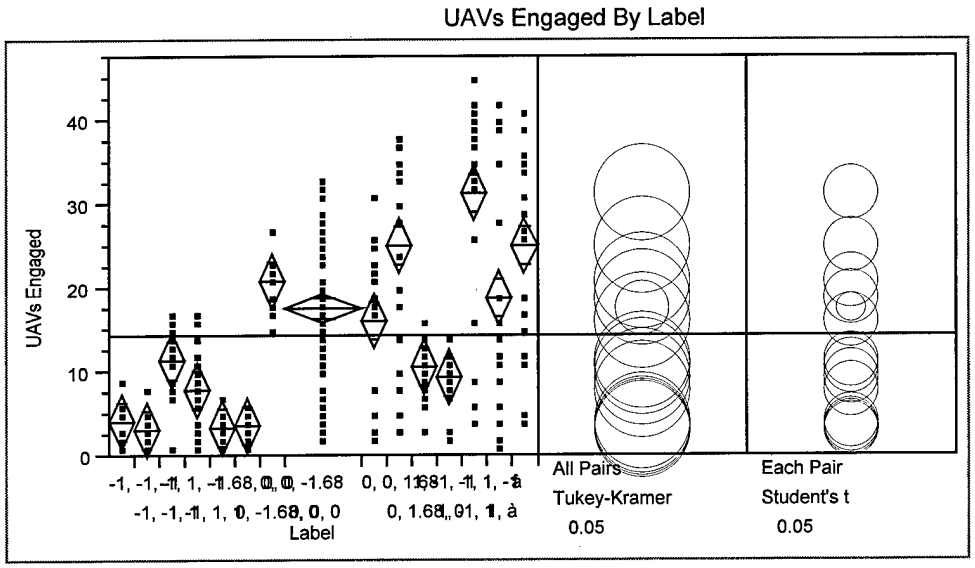

Figure 14: Tukey-Kramer Multiple Comparison Procedure for Number of UAVs Engaged (SEAD)

Screening Fit
UAVs Engaged
Summary of Fit

RSquare	0.722078
RSquare Adj	0.715361
Root Mean Square Error	6.039078
Mean of Response	14.35294
Observations (or Sum Wgts)	340

Analysis of Variance

Source	DF	Sum of Squares	Mean Square	F Ratio
Model	8	31363.922	3920.49	107.4977
Error	331	12071.725	36.47	Prob>F
C Total	339	43435.647		<.0001

Figure 15: Response Model for Number Times UAV Engaged (SEAD Study)

The number of times the UAV is engaged increases as both the probability of detection and the number of threats increase. We expect that threat lethality would not be significant, since the UAV must be engaged before the threat affects it in the simulation. However, counter-intuitively we find a decreasing effect. This is again due to UAV destruction and subsequent replication termination. As the lethality increases, UAVs tend to be destroyed earlier and therefore are capable of fewer engagements.

Screening Fit
UAV Engaged
Summary of Fit

RSquare	0.989087
RSquare Adj	0.978175
Root Mean Square Error	1.266616
Mean of Response	14.35294
Observations (or Sum Wgts)	17

Analysis of Variance

Source	DF	Sum of Squares	Mean Square	F Ratio
Model	8	1163.2928	145.412	90.6378
Error	8	12.8345	1.604	Prob>F
C Total	16	1176.1274		<.0001

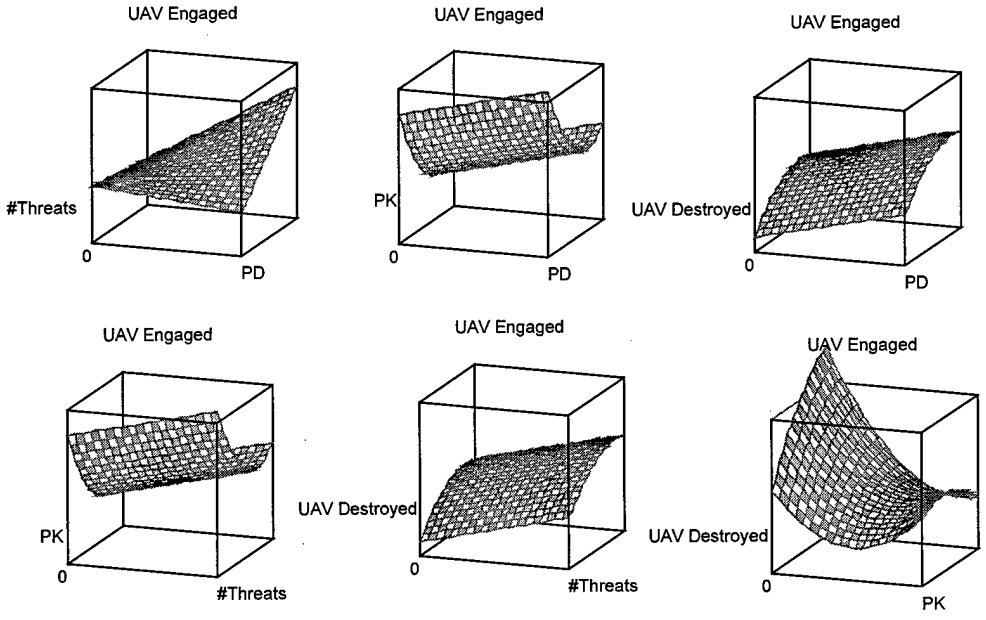

Figure 16: Response Surface for Average Number Times UAV Engaged (SEAD Study)

Percentage of Mission Accomplished. The 90% confidence intervals for the percent of mission accomplished and the Tukey-Kramer results are shown in Figures 17and 18, respectively. We find only a few of the points show a statistical difference in the response. Nevertheless, we construct the response surface to see if any impacts are visible (Figure 19). The R^2 for the model is 0.91, but once again we have non-normal residuals, thereby preventing any definite effects predictions. Nevertheless, we do see from this model that a significant portion of the error is explained by the regressors.

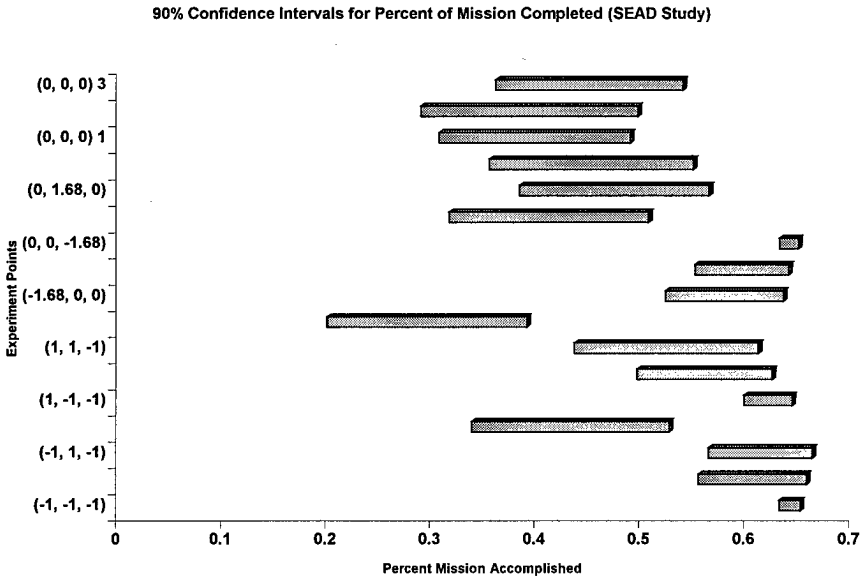

Figure 17: Confidence Intervals for the Percent of Mission Accomplished (SEAD Study)

As we expect from the confidence intervals, there is very little change in the response over most of the region. However, we see a slight increase in percent mission accomplished at the four corner points of the region. Because of the deviation from the

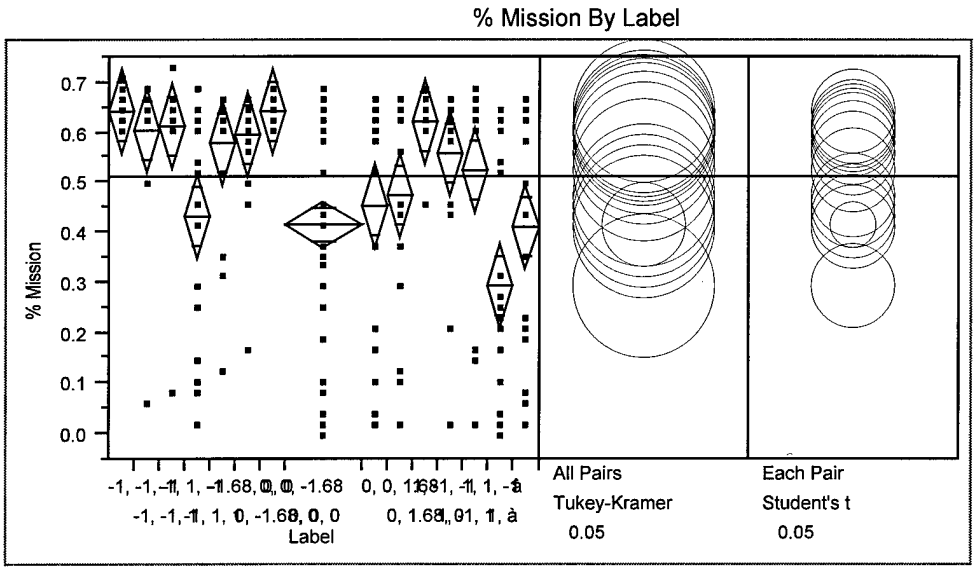

Figure 18: Tukey-Kramer Multiple Comparison Procedure for Percent Mission Accomplished (SEAD)

normality assumption, we conduct both Kruskal-Wallis and median non-parametric tests that indicate that there is a indeed a statistical difference between the points. The interaction between UAVs engaged and both probability of detection and number of threats is curious. While the percent mission accomplished increases with number of engagements (which seems counter-intuitive), it is again a result of the replication terminating on UAV destruction. More engagements correspond to the UAV remaining in the replication longer and therefore covering more targets. This is confirmed by the reduction in mission accomplishment at a given level of engagements as probability of detection and number of threats is increases. Again, to fully understand the relationship between number of engagements and percent mission accomplishment, a study of multiple UAVs is warranted. We present a summary of our observations in Table 3.

Screening Fit
% Mission
Summary of Fit

RSquare	0.914164
RSquare Adj	0.910741
Root Mean Square Error	0.064101
Mean of Response	0.511029
Observations (or Sum Wgts)	340

Analysis of Variance

Source	DF	Sum of Squares	Mean Square	F Ratio
Model	13	14.265843	1.09737	267.0727
Error	326	1.339498	0.00411	Prob>F
C Total	339	15.605341		<.0001

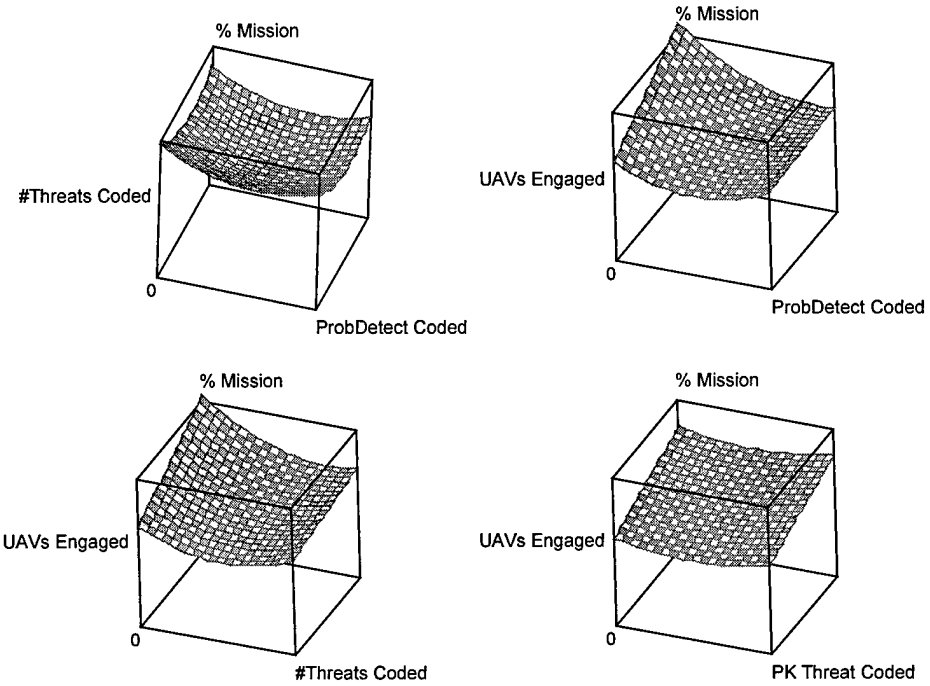

Figure 19: Response Surface for the Percent of Mission Accomplished (SEAD Study)

Table 3: Summary of SEAD Observations

SEAD Study	
MOE	Attractive Region
# UAVs Destroyed	Low #Threats, Probability of Detection, & Low Lethality
# Times Engaged	Low Probability of Detection & Low #Threats
% Mission Accomplished	No Statistically Significant Conclusions

II.4.3 Scenario 2--UAV Performance

The UAV Performance portion of this research uses the model to predict the operational effect of changes to Predator performance parameters. By operational effect we mean changes to the capability of the Predator to perform both its current surveillance mission and potential Active SEAD mission. The changes to aircraft aerodynamic and performance characteristics and their corresponding effect on MOEs are listed in Table 5 and the design matrix is shown in Table 4. For the surveillance mission, we assume negligible threats. For the Active SEAD mission, we assume 10 threats that have a probability of detecting the UAV of 0.5, ranges of 10 nm (6 threats) and 20 nm (4 threats), and probabilities of kill of 1% (4 threats), 2% (3 threats), and 3% (3 threats).

Table 4: UAV Performance Design Matrix

	Coded Point		Uncoded Point	
	Speed (knots)	Endurance (hours)	Speed (knots)	Endurance (hours)
Corner Points	-1	-1	65	10
	-1	1	65	20
	1	-1	200	10
	1	1	200	20
Axial Points	-1.4	0	37	15
	0	-1.4	132.5	7.9
	1.4	0	228	15
	0	1.4	132.5	22.1
Center Points	0	0	132.5	15
	0	0	132.5	15
	0	0	132.5	15

Table 5: UAV Characteristics and MOEs

UAV Characteristics	Measures of Effectiveness
Surveillance Mission	Surveillance Mission
Air Speed	Coverage (Covered / Planned)
Susceptibility to weather	Number of Targets Covered
Endurance	Percentage of Time Spent in Route
Active SEAD Mission	Active SEAD Mission
Airspeed	Number of UAVs Destroyed
Endurance	Number of UAVs Engaged
	Percentage of Mission Accomplished

Coverage (Surveillance Mission). The 90% confidence intervals for coverage are shown in Figure 20 and the Tukey-Kramer results in Figure 21. There is a statistically significant difference between most design points. The response surface for coverage is

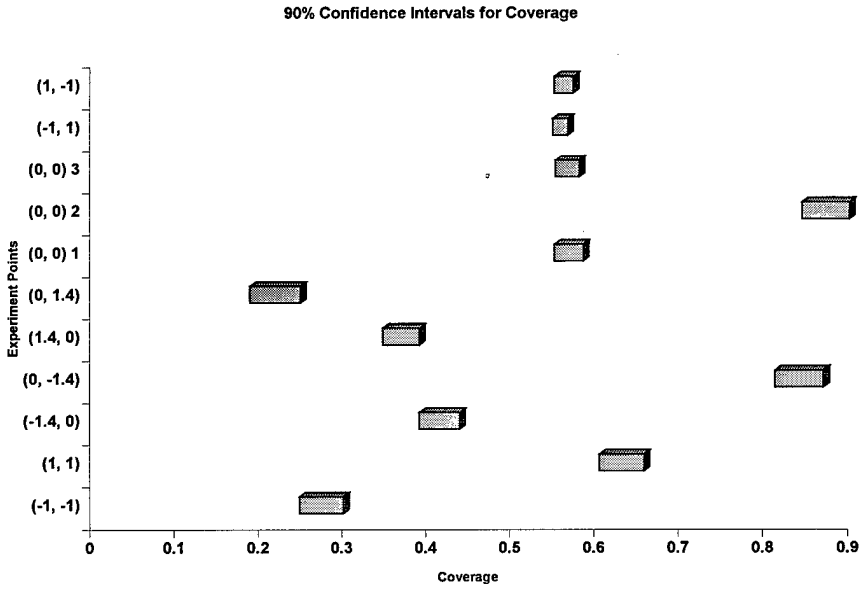

Figure 20: 90% Confidence Intervals for Coverage

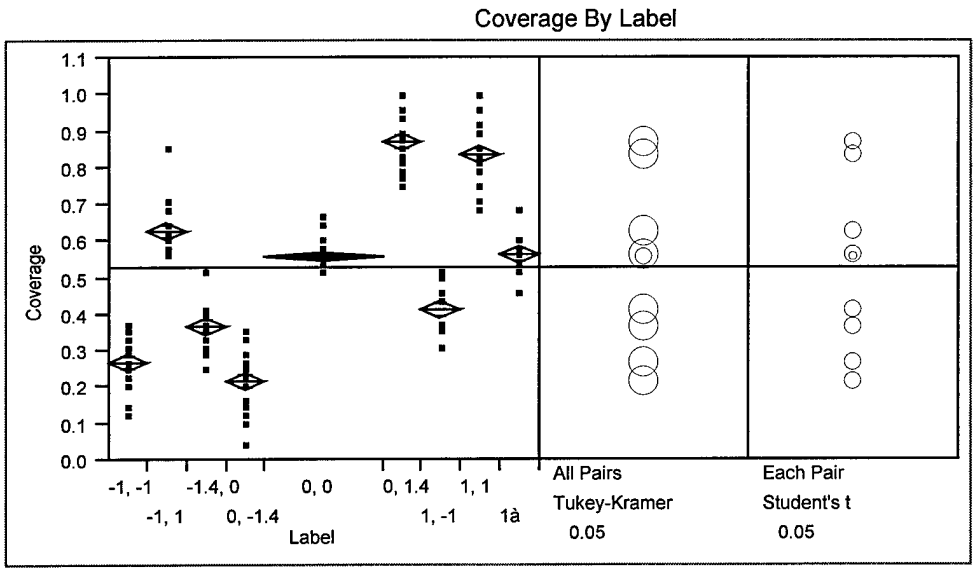

Figure 21: Tukey-Kramer Multiple Comparison Procedure for Coverage

Screening Fit
Coverage
Summary of Fit

RSquare	0.911079
RSquare Adj	0.909425
Root Mean Square Error	0.06216
Mean of Response	0.53125
Observations (or Sum Wgts)	220

Analysis of Variance

Source	DF	Sum of Squares	Mean Square	F Ratio
Model	4	8.5117119	2.12793	550.7219
Error	215	0.8307360	0.00386	Prob>F
C Total	219	9.3424479		<.0001

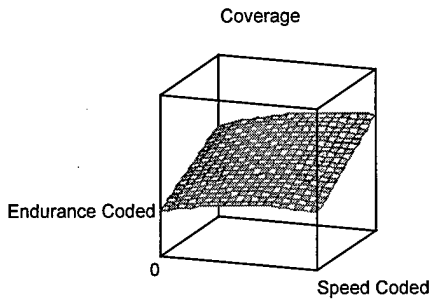

Figure 22: Response Surface for Coverage

shown in Figure 22. The R^2 for this model is 0.91. Again, we have residuals that are slightly non-normal. But, we can say that a significant portion of the variability of the response is due to the controls. Conducting Kruskal-Wallis and median non-parimetric tests, we verify the results of the Tukey-Kramer test. The response increases with both controls and we achieve the greatest increase in coverage at high speeds and high endurance.

Percent Time in Route. (Surveillance Mission). The 90% confidence intervals for percent time in route and the Tukey-Kramer Results are shown in Figures 23 and 24. Again, there is a statistically significant difference between almost all of the design points. The response surface is shown in Figure 25. The R^2 for this model is 0.93 and we

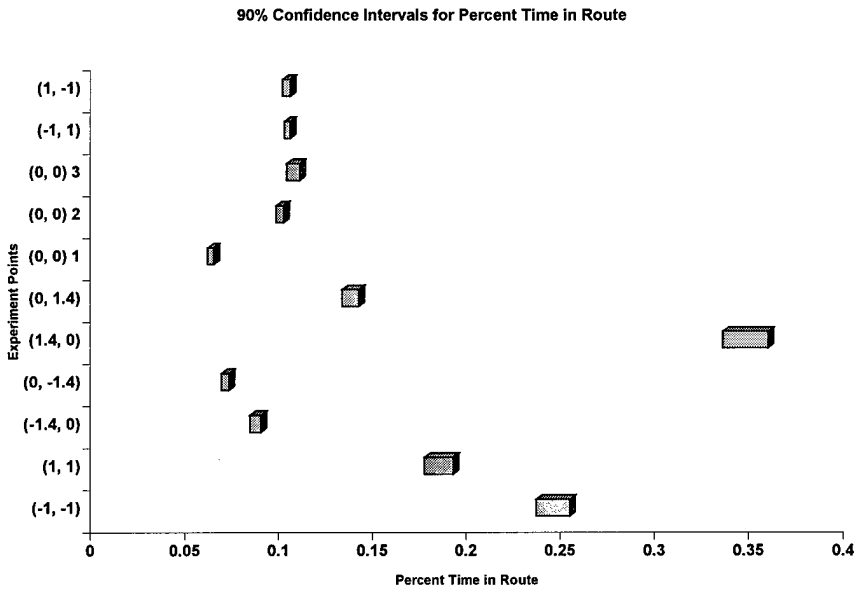

Figure 23: 90% Confidence Intervals for Percent Time in Route

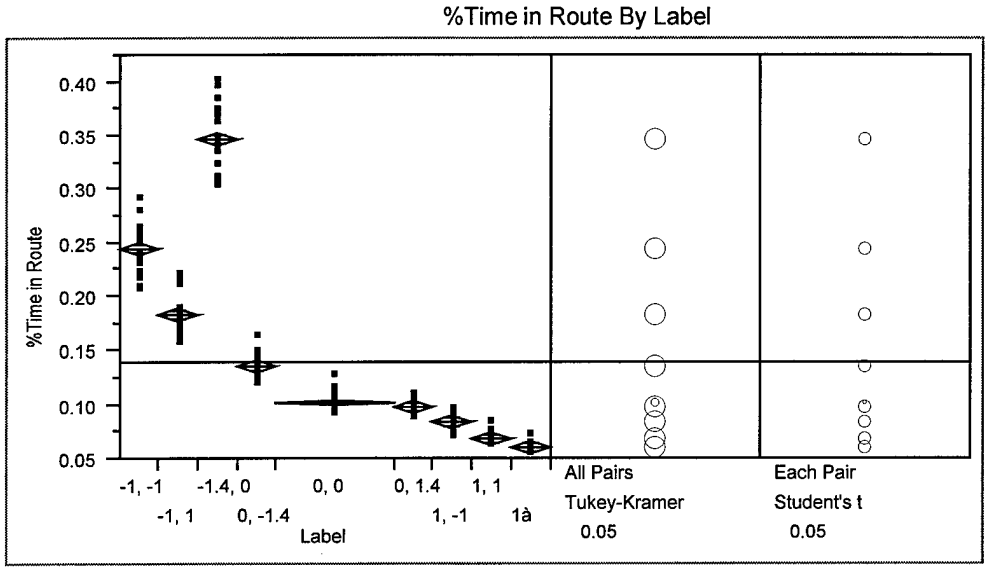

Figure 24: Tukey-Kramer Multiple Comparison Procedure for Percent Time in Route

Screening Fit
%Time in Route
Summary of Fit

RSquare	0.934809
RSquare Adj	0.933596
Root Mean Square Error	0.021641
Mean of Response	0.139508
Observations (or Sum Wgts)	220

Analysis of Variance

Source	DF	Sum of Squares	Mean Square	F Ratio
Model	4	1.4438786	0.360970	770.7443
Error	215	0.1006929	0.000468	Prob>F
C Total	219	1.5445715		<.0001

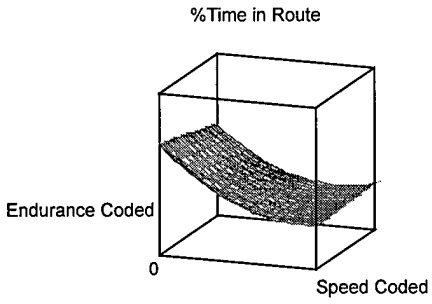

Figure 25: Response Surface for Percent Time in Route

have residuals that are slightly non-normal. But, as before, we can say that a significant portion of the variability of the response is due to the controls. And again conducting the Krasal-Wallis and median tests, we verify the Tukey-Kramer results. From the response surface, we see that most of the response appears due to changes in the input variable speed.

Number of UAVs Destroyed (SEAD Mission). The 90% confidence interval for the average number of UAVs destroyed at each design point is shown in Figure 26. The Tukey-Kramer test results are shown in Figure 27. We find a statistically significant difference at only two pairs of the design points.

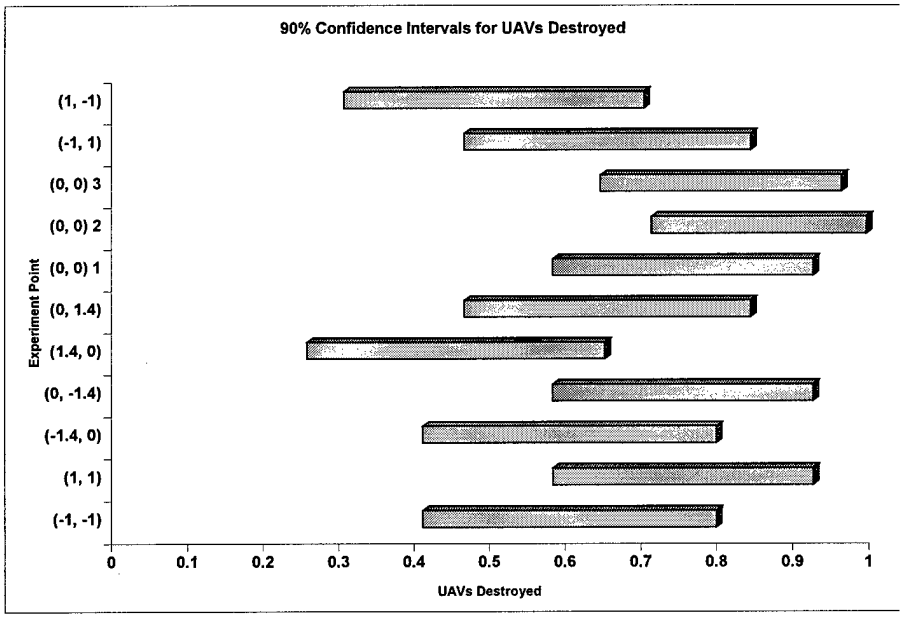

Figure 26: 90% Confidence Intervals for Number of UAVs Destroyed (Performance)

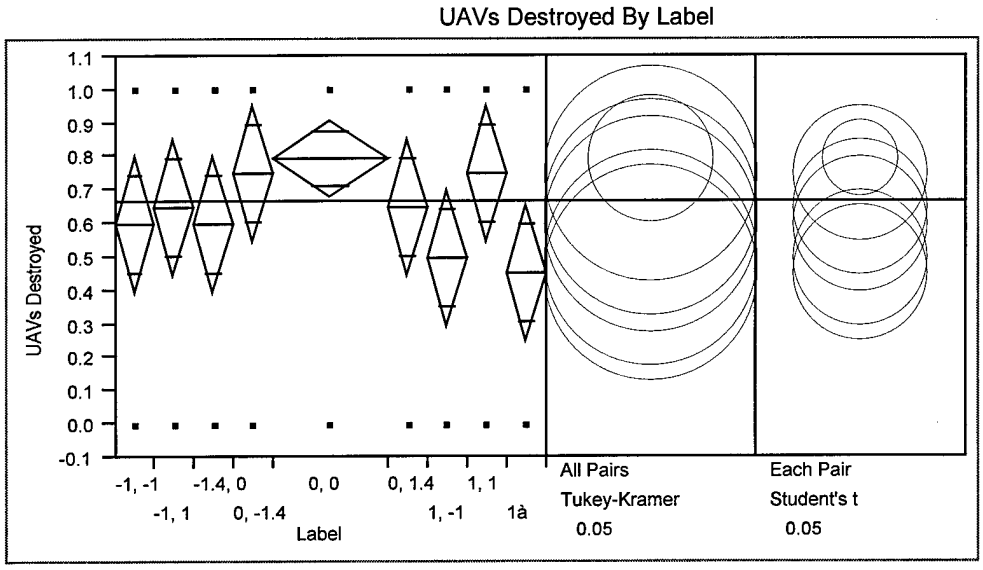

Figure 27: Tukey-Kramer Multiple Comparison Procedure for Number UAVs Destroyed (Performance)

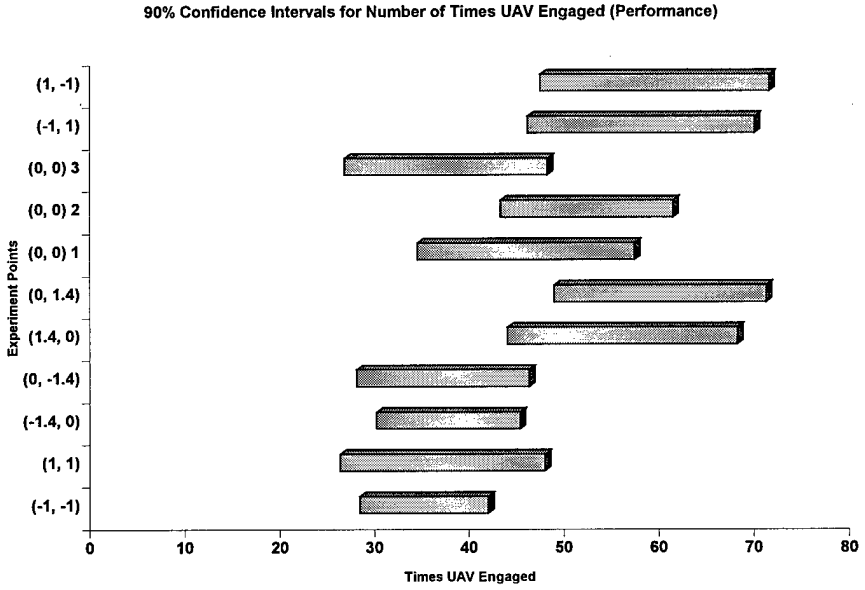

Figure 28: 90% Confidence Intervals for Number of Times UAV Engaged (Performance)

Number of UAVs Engaged (SEAD Mission). The 90% confidence intervals for the number of times the UAV is engaged per mission is shown in Figure 28 and the Tukey-Kramer results in Figure 29. We find that there is a statistical difference in the average response at most of the design points. Again, to investigate the response, we

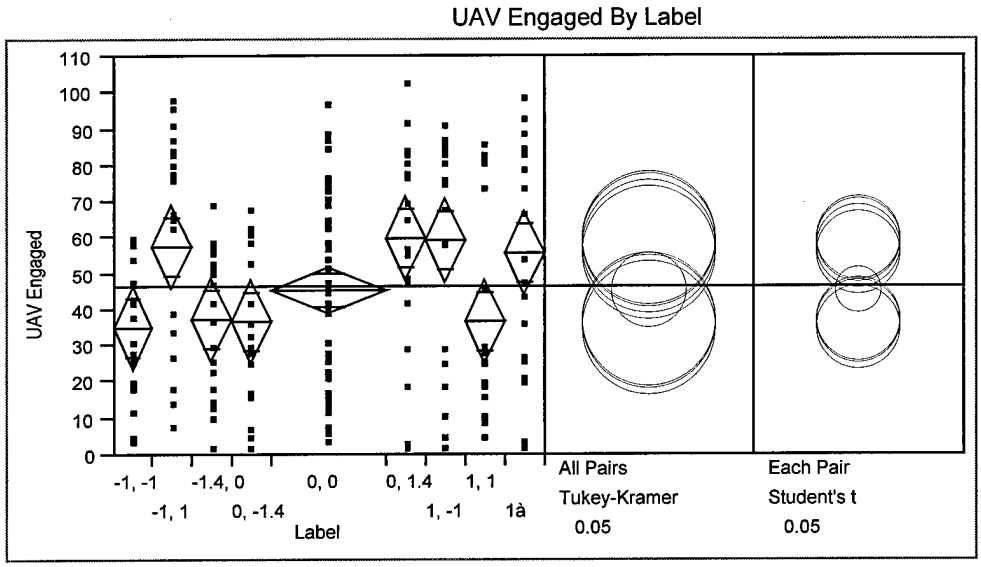

Figure 29: Tukey-Kramer Multiple Comparison Procedure for Number UAVs Engaged (Performance)

Screening Fit
UAV Engaged
Summary of Fit

RSquare	0.533316
RSquare Adj	0.517833
Root Mean Square Error	19.48779
Mean of Response	46.72603
Observations (or Sum Wgts)	219

Analysis of Variance

Source	DF	Sum of Squares	Mean Square	F Ratio
Model	7	91573.24	13081.9	34.4465
Error	211	80132.32	379.8	Prob>F
C Total	218	171705.56		<.0001

Figure 30: Response Model for Number Times UAV Engaged (Performance)

construct a response model shown in Figure 30. R^2 for this model is 0.53. However, the residuals are normal. As in the Active SEAD study, we construct an additional response surface of the average number of engagements per design point (Figure 31). R^2 for this model is 0.897, but the residuals are not normally distributed.

Screening Fit
UAVs Engaged
Summary of Fit

RSquare	0.89682
RSquare Adj	0.742051
Root Mean Square Error	5.255123
Mean of Response	46.58636
Observations (or Sum Wgts)	11

Analysis of Variance

Source	DF	Sum of Squares	Mean Square	F Ratio
Model	6	960.1452	160.024	5.7946
Error	4	110.4653	27.616	Prob>F
C Total	10	1070.6105		0.0554

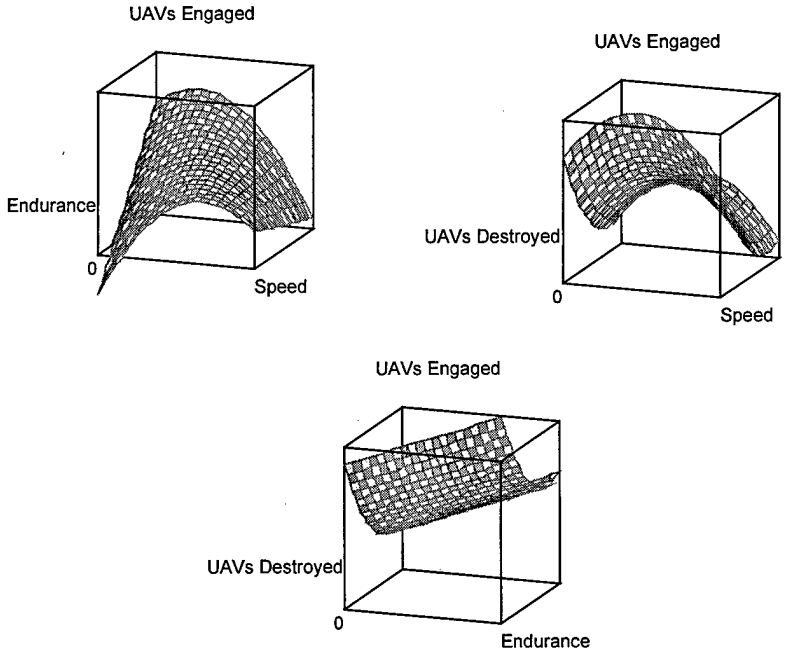

Figure 31: Response Surface for Average Number Times UAV Engaged (Performance)

As before, we verify the results of the Tukey-Kramer test with the Kruskal-Wallis and median tests which verify a statistical difference between design points. The number of times the UAV is engaged appears to be lowest in the high speed at any endurance and low speed, low endurance areas of the test regime. The effect of low endurance can be explained in that the chance of engagement increases the longer the UAV is in theater. We note that there is no parameter in the simulation which makes the threats more or less lethal or likely to detect a UAV based on speed. The affect of speed is due to the choice of routes made by the routing algorithm.

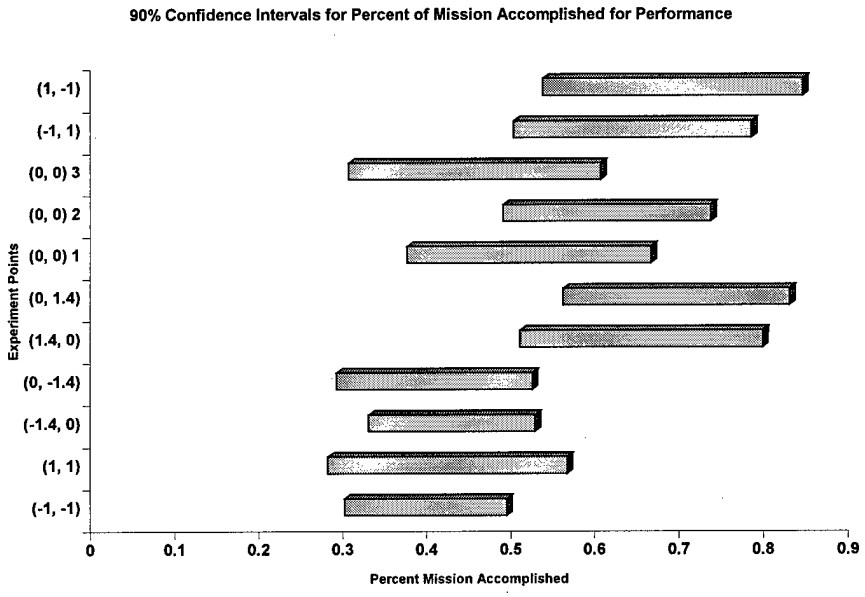

Figure 32: Confidence Intervals for the Percent of Mission Accomplished (Performance)

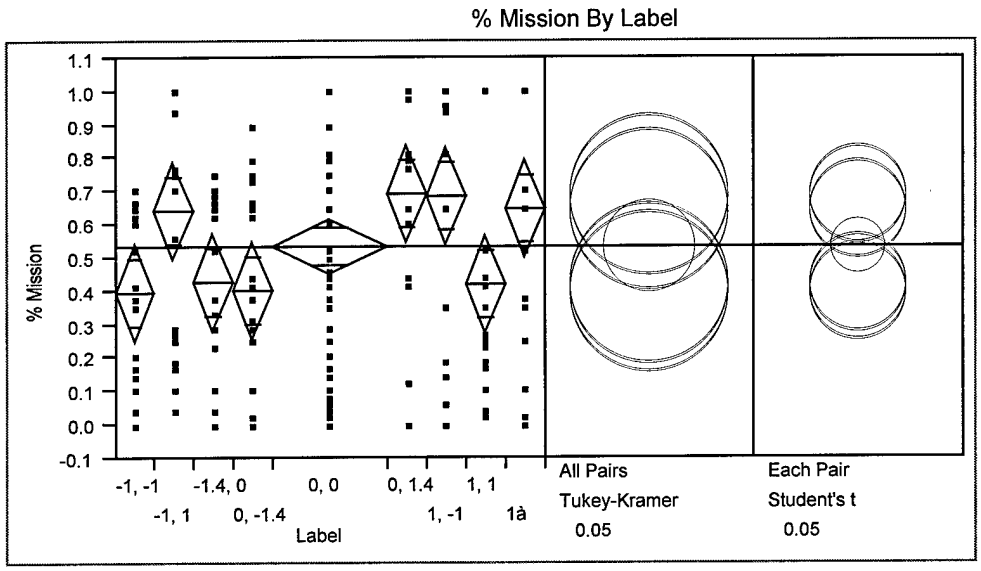

Figure 33: Tukey-Kramer Multiple Comparison Procedure for Percent Mission Accomplished (Performance)

Table 6: Summary of Performance Observations

Performance Study	
Mission: Surveillance MOE	 Attractive Region
Coverage % Time in Route	High Speed, High Endurance High Speed
Mission: Active SEAD MOE	 Attractive Region
# UAVs Destroyed # Times Engaged % Mission Accomplished	No Statistically Significant Conclusions Low Speed, Low Endurance High Speed, High Endurance Low Speed, Mid Endurance Mid Speed, Low Endurance Response not affected by Control Variables

Percentage of Mission Accomplished (SEAD Mission). The 90% confidence intervals for the percent of mission accomplished are shown in Figure 32 and Tukey-

Kramer results in Figure 33. Again, we find that there is a statistical difference in the average response at several of the design points. The constructed response surface is shown in Figure 34. The R^2 for the model is 0.97, and the model meets the assumptions of normality.

Screening Fit
% Mission
Summary of Fit

RSquare	0.966613
RSquare Adj	0.965175
Root Mean Square Error	0.066201
Mean of Response	0.537386
Observations (or Sum Wgts)	219

Analysis of Variance

Source	DF	Sum of Squares	Mean Square	F Ratio
Model	9	26.518827	2.94654	672.3275
Error	209	0.915961	0.00438	Prob>F
C Total	218	27.434789		<.0001

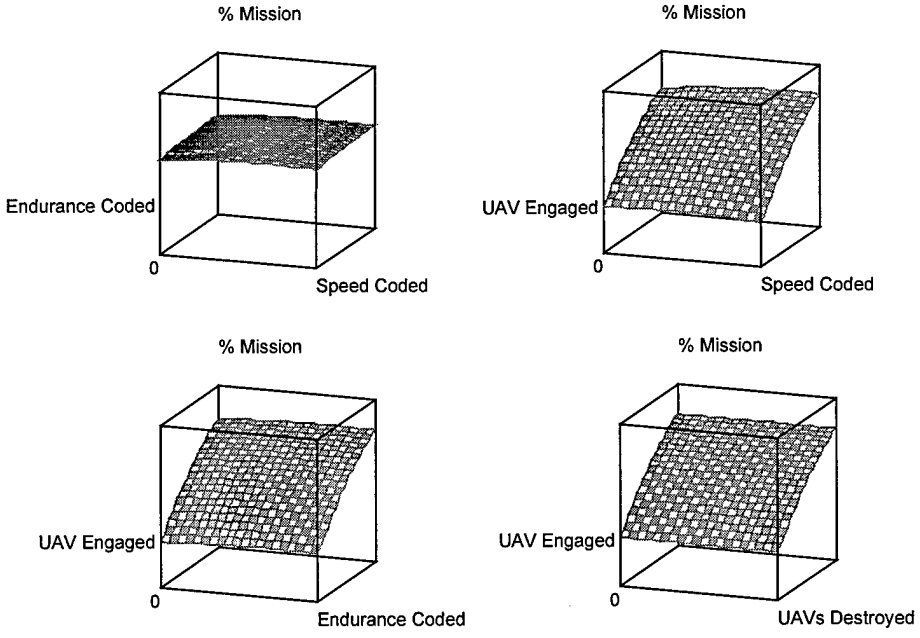

Figure 34: Response Surface for the Percent of Mission Accomplished (Performance)

The response surface appears unaffected by the two control variables. The response seems most affected by the number of UAV engagements. Again, this is likely due to the UAV termination issue. Another area of further investigation would be to include threat penalties in the routing algorithm. With that and multiple UAVs, a clearer interpretation of the interaction of engagements and mission accomplishment could be ascertained. We present a summary of our observations in Table 6.

II.5. Conclusions

Because the use of UAVs in military operations is expected to continue its increase, so will the necessity for not only new tactics and techniques, but also efficient and cost effective ways to test them. Simulation is one such method. Simulation cannot by itself prove operational acceptability, but can provide a means to filter to proposed initiatives. We demonstrated this use of simulation by the creation of a discrete event simulation for the Predator and its use with two Kenney Battlelab initiatives, Active SEAD and UAV Performance. We provided a working prototype and initial analysis to the UAVB and USAFA.

Appendix A

RQ-1A Predator

Mission Need Statement: "Endurance UAV systems provide a broad spectrum of intelligence collection capability to support joint combatant forces in worldwide peace, crisis, and wartime operations. The capabilities of these UAV systems will provide information for adaptive real-time planning of current operations, to include: monitoring enemy offensive and defensive positions, deception postures and combat assessment. Endurance UAVs will provide a rapid turnaround of raw data to aid a robust targeting cycle following a 'First Look, First Shoot, First Kill' methodology." (USAF ACC, 1998b: Sect. 2.1)

Tasks: Near-Real time (NRT) Targeting and Precision Strike Support, NRT Combat Assessment, Enemy Order of Battle (EOB) Information, Battle Damage Assessment (BDA), Intelligence Preparation of the Battlefield (IPB), Special Operations Support, Blockade and Quarantine Enforcement, Sensitive Reconnaissance Operations (SRO), Humanitarian Aid, United Nations (UN) Treaty Monitoring, Counter Drugs, Single Integrated Operational Plan (SIOP), and Communications. (USAF ACC, 1998b: Sect. 2.2.1 to 2.2.13)

Capabilities: Semi autonomous, dynamically retaskable, low to medium altitude, long endurance UAV providing near-continuous coverage (75% ETOS) within a 400 NM operational radius using simultaneous carriage of electro-optical (EO), infrared (IR), and

synthethic aperture radar (SAR) sensors at altitudes up to 25,000 ft. The baseline system demonstrated a 20-hour total flight time capability at 13,000 MSL. (USAF ACC, 1998b: Sect. 2.4.1)

Characteristics:

Table A-1: Predator Characteristics (USAF ACC, 1998b: table 2-4)

Gross Take-off Weight	>1873 lbs (EO/IR)
Wingspan	48.7 ft
Mission Duration/Operating Radius	20 hrs on station @ 400 NM
Maximum Endurance	40 hrs
Payload	>450 lbs
True Air Speed	60-105 kts
Loiter Altitude	25,000 ft max. 15,000 ft nominal
Survivability Measures	None
Command and Control	Ku band SATCOM C band LOS
Sensors	SAR: 1ft IPR, Swath Width Approx. 800m EO: NIIRS 7 IR: NIIRS 5 Simultaneous Dual Carriage
Coverage per Mission	13,000 sq NM search imagery
Sensor Data Transmission	Ku band: 1.5Mb/sec LOS: C band 4.5Mb/s
Deployment	3 C-141s or 7 C-130s 2/C-5/C-17
Ground Control Station	LOS & OTH
Data Exploitation	Existing and Programmed: DoD CIG/SS compliant processing systems

Platform Threats: Because of its operating envelope (nominal altitude and indicated airspeed of 15,000 ft and 65 knots respectively), the Predator is vulnerable to a variety of threats including: radio-frequency and infrared guided surface-to-air missiles (SAM); anti-aircraft artillery (AAA); and second, third, and fourth generation combat equipped

with air-to-air missiles, guns, and rockets. Additionally, while operating at an altitude of 5,000 ft, other threats include: unsophisticated, visually acquired AAA and man-portable SAM systems. The Predator does not contain an onboard electronic attack (EA) system. (USAF ACC, 1998b: Sect. 1.6.1)

Electromagnetic Spectrum Threats: Electromagnetic spectrum threats include active and passive detection capability that would enable target area concealment and deception activity; systems that could threaten the transmission of collected data; and communication link interception, jamming, or corruption.

Appendix B

Wind Correction

To calculate the time between targets, the simulation requires the ground trace and speed of the UAV. As shown in Figure B-1, the UAV heading must be corrected for winds aloft. The change in the heading changes the direction of the true airspeed. This change in the true airspeed vector and the wind vector affect the groundspeed of the UAV. The reduced (or increased) groundspeed of the UAV affects the simulation parameters. The simulation requires the groundspeed to calculate the time between targets (for event scheduling). The simulation uses the vector arithmetic shown in Figure B-2 to combine the true airspeed and windspeed.

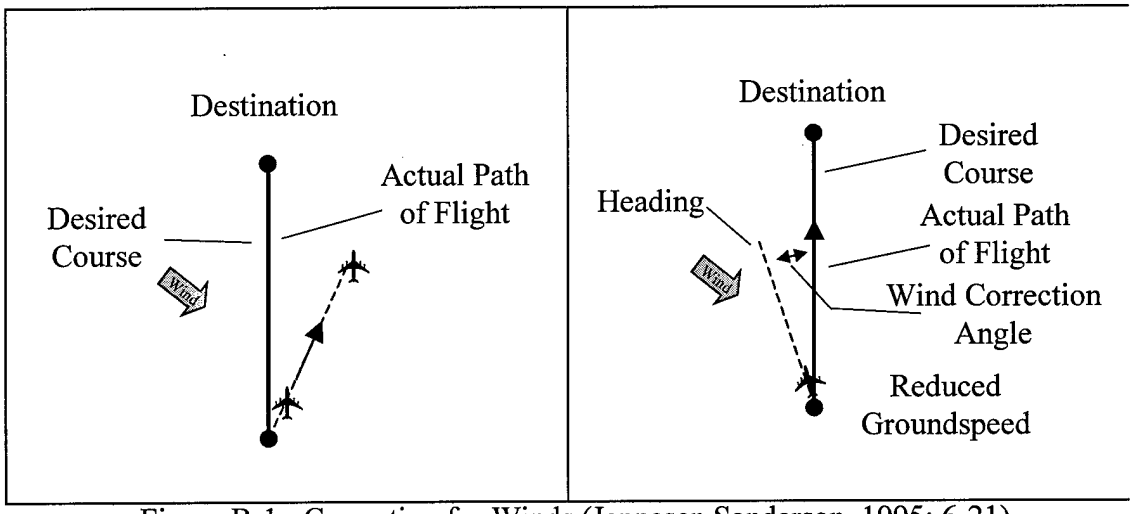

Figure B-1: Correction for Winds (Jeppesen Sanderson, 1995: 6-21)

$$\theta_{Truecourse} = \tan^{-1}\left[\frac{Y_T - Y_F}{X_T - X_F}\right]$$

$$\beta = \theta_{wind} - \theta_{TrueCourse}$$

$$\beta = \theta_{wind} - \tan^{-1}\left[\frac{Y_T - Y_F}{X_T - X_F}\right]$$

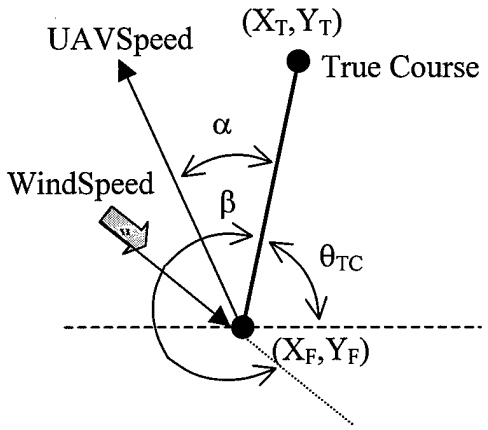

Figure B-2: Wind Correction Equations Part I

As shown in figure B-2 above, the angle between the wind vector and the UAV true course can be found by subtracting the inverse tangent of the coordinate differences of true course vector from the angle of the wind vector. As we know, for the UAV to traverse the true course, the projection of the wind perpendicular the true course must equal the projection of the UAV speed perpendicular to the true course. This is shown below in Figure B-3.

$$Projection WindSpeed \perp TrueCourse = Projection UAVSpeed \perp TrueCourse$$

$$WindSpeed * \sin\beta = UAVSpeed * \sin\alpha$$

$$\alpha = \sin^{-1}\left[\frac{WindSpeed * \sin\beta}{UAVSpeed}\right]$$

$$\alpha = \sin^{-1}\left[\frac{WindSpeed * \sin\left[\theta_{Wind} - \tan^{-1}\left(\frac{Y_T - Y_F}{X_T - X_F}\right)\right]}{UAVSpeed}\right]$$

Figure B-3: Wind Correction Equations Part II

Then we can calculate α, the angle between the true course and the heading (UAV speed vector) as shown above. It then follows that the UAV speed along the true course is the projection of the UAV speed onto the true course plus the projection of the wind speed onto the true course. This is shown in Figure B-4.

$$Speed_{TrueCourse} = Projection UAVSpeed \angle TrueCourse + Projection WindSpeed \angle TrueCourse$$

$$Speed_{TrueCourse} = UAVSpeed * \cos\alpha + WindSpeed * \cos\beta$$

$$Speed_{TrueCourse} = UAVSpeed * \cos\left\{\sin^{-1}\left[\frac{WindSpeed * \sin[\theta_{Wind} - \theta_{TC}]}{UAVSpeed}\right]\right\} + WindSpeed * \cos\{\theta_{wind} - \theta_{TC}\}$$

Figure B-4: Wind correction Equations Part III

Distance Conversion from Latitude/Longitude to Cartesian Coordinates:

To convert between the two coordinate systems, we use existing methods in the routing algorithm (O'Rourke: 1999) to determine the distance between a point and the origin, and the angle between true north and line connecting the point and the origin. We consider true north to be the Y-axis in our Cartesian coordinate system. The Cartesian Coordinates are then calculated as shown in Figure B-5:

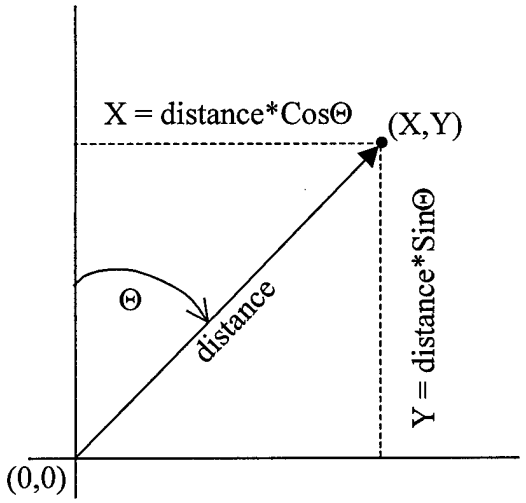

Figure B-5: Conversion to Cartesian Coordinates

Appendix C

Weather Model—Probability Data

CLIMATOLOGICAL DATA FOR KOSOVO

PERIOD OF RECORD: 1973 TO 1998

1. These data were computed using surface observations taken at Pristina, Yugoslavia; Tuzla, Croatia; and Skopje, Macedonia during the above period of record. Upper air climatology were computed from Zagreb, Croatia soundings for the same period of record.

2. The surface observation count at Skopje was the best: 168,422. The ob count for Pristina and Tuzla respectively was 30,664 and 15,476. The count for the upper data from Zagreb was 15,151 soundings.

3. The ZAGREB ICING sheet contains percentage frequencies for the requested icing categories, and frequencies of the occurrence of any icing in three 10,000-foot layers. In the top table, multiple icing conditions within a 10,000 foot layer were treated as a single occurrence. In the bottom table, whenever a certain intensity of icing occurs anywhere from the surface to 30,000 feet, it is counted. Multiple light icing conditions only count as one occurrence of light icing per sounding, however. These differences in the computation of frequencies account for the apparent discrepancies between the two tables. The algorithm used to compute these statistics does not take advection or cloud cover into account. Instead it is based solely on the temperature, dew point, relative humidity, and lapse rate for a single sounding. The resultant data are pessimistic and only indicate that favorable conditions for icing exist.

4. The ZAGREB TURBC sheet contains percentage frequencies for the requested turbulence categories, and frequencies of the occurrence of any turbulence with an intensity of LGT-MDT (light, occasional moderate) or greater in three 10,000-foot layers. In the top table, multiple turbulence conditions within a 10,000 foot layer were treated as a single occurrence. In the bottom table, whenever a certain intensity of turbulence (LGT-MDT or greater) occurs anywhere from surface to 30,000 feet, it is counted. These statistics were computed the same way as the icing statistics. The algorithm used to compute these statistics was derived from AFGWC TN 79/001 (Clear Air Turbulence Forecasting Techniques), and only looks at conditions favorable for clear air turbulence from a single sounding (using wind speed, stability, and vector wind shear). The resultant data are optimistic, because the algorithm does not include conditions favorable for mechanical low level turbulence due to rough terrain.

5. The ZAGREB UA TEMPS sheet contains percentage frequencies for each mission impact category on the requested upper air temperature conditions. The data show that the atmosphere is indeed warmer in the summer months and cooler in the winter months.

6. The SURFACE PARAMETERS sheet contains the percentage frequencies for all parameters (combined) that can be derived from HOURLY surface observations. Upper air soundings are taken every 6 or 12 hours, so the upper air statistics could not be grouped with surface observation statistics. The high occurrence of UNFAVORABLE conditions is due to the high occurrence of sky cover > 50 percent. If this factor were eliminated, the UNFAVORABLE frequency would be much lower.

7. The CEILING sheet contains percentage frequencies for the requested ceiling categories.

8. The CROSSWINDS sheet contains percentage frequencies for the requested crosswind categories at the 3 airfields. Crosswind components were computed from these runway headings: Pristina 35/17 Skopje 34/16 Tuzla 27/09.

9. The SKY COVER sheet contains percentage frequencies for the requested sky cover categories.

10. The VISIBILITY sheet contains percentage frequencies for the requested visibility categories from surface observations.

11. The WIND SPEED sheet contains the percentage frequencies for the requested average (or sustained) wind speed categories from surface observations.

ZAGREB, CROATIA

FREQUENCY OF ICING BY 10,000 FT LAYERS
PERIOD OF RECORD: 1973 TO 1998

MONTH	FREQ OF ICG 0 TO 10K FEET	FREQ OF ICG 10K TO 20K FEET	FREQ OF ICG 20K TO 30K FEET	OB COUNT
JAN	3.6%	1.5%	0.0%	1228
FEB	3.2%	2.2%	0.0%	1217
MAR	3.7%	2.5%	0.0%	1394
APR	2.4%	2.9%	0.1%	1356
MAY	1.2%	2.5%	0.5%	1304
JUN	2.0%	7.1%	2.0%	1281
JUL	0.8%	13.7%	4.8%	1383
AUG	0.6%	13.3%	5.7%	1294
SEP	3.6%	10.0%	3.3%	1195
OCT	2.4%	4.7%	1.1%	1158
NOV	3.0%	2.9%	0.2%	1121
DEC	5.4%	3.0%	0.0%	1220

PERCENTAGE FREQUENCIES FOR CATEGORIES OF ICING
SFC TO 30,000 FT

MONTH	FAVORABLE NO ICING	MARGINAL TRACE/LGT ICING	UNFAVORABLE MDT/SVR ICING
JAN	87.5%	10.6%	2.0%
FEB	90.6%	8.1%	1.3%
MAR	87.4%	10.2%	2.4%
APR	88.9%	9.9%	1.3%
MAY	92.2%	6.7%	1.1%
JUN	79.2%	16.6%	4.2%
JUL	64.6%	27.6%	7.7%
AUG	63.9%	29.1%	7.0%
SEP	71.7%	22.9%	5.4%
OCT	84.1%	13.1%	2.8%
NOV	87.2%	11.4%	1.3%
DEC	81.3%	16.1%	2.5%

ZAGREB, CROATIA

FREQUENCY OF CLEAR AIR TURBULENCE BY 10,000 FT LAYERS
(ANY C.A.T. WITH INTENSITY LGT-MDT OR GREATER)
PERIOD OF RECORD: 1973 TO 1998

MONTH	FREQ OF TURBC 0 TO 10K FEET	FREQ OF TURBC 10K TO 20K FEET	FREQ OF TURBC 20K TO 30K FEET	OB COUNT
JAN	0.6%	1.7%	3.9%	1420
FEB	0.3%	1.3%	4.4%	1388
MAR	0.2%	1.3%	3.3%	1501
APR	0.3%	1.1%	2.3%	1432
MAY	0.3%	0.2%	1.7%	1370
JUN	0.2%	0.6%	1.1%	1336
JUL	0.1%	0.5%	1.4%	1439
AUG	0.2%	0.7%	1.1%	1336
SEP	0.2%	0.6%	0.9%	1245
OCT	0.3%	1.0%	1.7%	1242
NOV	0.4%	0.6%	2.8%	1262
DEC	0.4%	1.7%	3.7%	1414

FREQUENCIES FOR CATEGORIES OF TURBULENCE
SFC TO 30,000 FT

MONTH	FAVORABLE NO / LGT TURBC	MARGINAL LGT-MDT TURBC	UNFAVORABLE >= MDT TURBC
JAN	94.6%	3.9%	1.4%
FEB	93.6%	4.4%	2.0%
MAR	95.1%	4.1%	0.8%
APR	95.8%	3.1%	1.0%
MAY	97.2%	2.0%	0.8%
JUN	97.8%	1.6%	0.7%
JUL	97.4%	1.7%	0.9%
AUG	97.8%	1.3%	0.9%
SEP	98.2%	1.4%	0.5%
OCT	97.1%	2.4%	0.5%
NOV	96.0%	2.5%	1.6%
DEC	94.0%	4.2%	1.8%

ZAGREB, CROATIA

FREQUENCY OF SPECIFIC TEMPS IN THE ATMOSPHERE
PERIOD OF RECORD: 1973 TO 1998

MONTH	FAVORABLE FL180 TEMP > -19C	MARGINAL <-19C BELOW FL180	UNFAVORABLE <-19C BELOW FL130
JAN	6.1%	69.7%	24.2%
FEB	6.2%	62.6%	31.2%
MAR	6.9%	68.0%	25.2%
APR	9.6%	75.6%	14.8%
MAY	49.4%	48.0%	2.6%
JUN	81.7%	17.6%	0.7%
JUL	90.7%	9.1%	0.2%
AUG	92.4%	7.5%	0.2%
SEP	84.1%	14.9%	1.0%
OCT	64.6%	31.3%	4.1%
NOV	28.6%	59.4%	12.0%
DEC	12.7%	69.6%	17.7%

PERCENTAGE FREQUENCIES FOR ALL SURFACE PARAMETERS COMBINED
PERIOD OF RECORD: 1973-1998

PRISTINA, YUGOSLAVIA

MONTH	FAVORABLE	MARGINAL	UNFAVORABLE
JAN	18.6%	9.9%	71.5%
FEB	27.1%	12.0%	60.9%
MAR	32.2%	10.7%	57.1%
APR	25.1%	11.2%	63.7%
MAY	23.9%	14.6%	61.5%
JUN	33.0%	17.6%	49.4%
JUL	50.2%	16.4%	33.3%
AUG	56.3%	14.3%	29.4%
SEP	48.1%	15.0%	36.9%
OCT	38.7%	12.1%	49.1%
NOV	22.3%	10.0%	67.7%
DEC	18.0%	11.1%	70.9%

SKOPJE, MACEDONIA

MONTH	FAVORABLE	MARGINAL	UNFAVORABLE
JAN	20.5%	7.5%	72.0%
FEB	31.5%	8.6%	59.9%
MAR	37.3%	8.4%	54.3%
APR	38.0%	12.0%	50.0%
MAY	40.0%	14.1%	45.9%
JUN	51.3%	15.6%	33.1%
JUL	63.7%	14.0%	22.3%
AUG	67.2%	11.5%	21.4%
SEP	62.4%	10.4%	27.1%
OCT	49.2%	8.4%	42.4%
NOV	27.7%	8.5%	63.8%
DEC	20.0%	6.6%	73.4%

TUZLA, BOSNIA-HERZEGOVINA

MONTH	FAVORABLE	MARGINAL	UNFAVORABLE
JAN	9.0%	11.2%	79.8%
FEB	15.9%	14.7%	69.4%
MAR	24.7%	12.5%	62.8%
APR	18.0%	14.6%	67.4%
MAY	18.8%	15.2%	66.1%
JUN	25.7%	19.4%	54.9%
JUL	36.5%	18.9%	44.6%
AUG	30.9%	18.0%	51.1%
SEP	28.2%	17.9%	53.8%
OCT	19.1%	16.8%	64.1%
NOV	8.2%	14.2%	77.6%
DEC	7.2%	13.7%	79.0%

PERCENTAGE FREQUENCIES FOR CATEGORIES OF CEILING
PERIOD OF RECORD: 1973-1998

PRISTINA, YUGOSLAVIA

MONTH	FAVORABLE CEILING > 2000 FT	MARGINAL CEILING 800-2000 FT	UNFAVORABLE CEILING < 800 FT
JAN	92.5%	1.1%	6.5%
FEB	97.0%	1.0%	2.1%
MAR	99.3%	0.6%	0.1%
APR	99.4%	0.4%	0.2%
MAY	99.6%	0.2%	0.2%
JUN	99.7%	0.1%	0.2%
JUL	99.9%	0.0%	0.1%
AUG	99.9%	0.1%	0.0%
SEP	99.4%	0.1%	0.4%
OCT	98.9%	0.2%	0.9%
NOV	94.7%	1.1%	4.3%
DEC	94.3%	1.4%	4.3%

SKOPJE, MACEDONIA

MONTH	FAVORABLE CEILING > 2000 FT	MARGINAL CEILING 800-2000 FT	UNFAVORABLE CEILING < 800 FT
JAN	82.0%	8.6%	9.4%
FEB	92.1%	5.6%	2.3%
MAR	97.0%	2.6%	0.4%
APR	98.9%	0.9%	0.2%
MAY	99.5%	0.4%	0.1%
JUN	99.8%	0.1%	0.1%
JUL	99.9%	0.1%	0.0%
AUG	99.9%	0.1%	0.0%
SEP	99.4%	0.4%	0.2%
OCT	98.0%	1.7%	0.4%
NOV	88.0%	7.2%	4.7%
DEC	77.3%	11.5%	11.1%

TUZLA, BOSNIA-HERZEGOVINA

MONTH	FAVORABLE CEILING > 2000 FT	MARGINAL CEILING 800-2000 FT	UNFAVORABLE CEILING < 800 FT
JAN	94.8%	1.6%	3.5%
FEB	97.5%	0.3%	2.3%
MAR	99.6%	0.1%	0.3%
APR	99.1%	0.1%	0.7%
MAY	99.1%	0.2%	0.7%
JUN	99.1%	0.2%	0.7%
JUL	99.6%	0.2%	0.3%
AUG	98.3%	0.5%	1.2%
SEP	97.7%	0.1%	2.2%
OCT	96.8%	0.3%	2.9%
NOV	96.1%	0.6%	3.3%
DEC	95.6%	0.3%	4.1%

PERCENTAGE FREQUENCIES FOR CATEGORIES OF CROSSWINDS
PERIOD OF RECORD: 1973-1998

PRISTINA, YUGOSLAVIA

MONTH	FAVORABLE CROSSWINDS < 10 KTS	MARGINAL CROSSWINDS 10-15 KTS	UNFAVORABLE CROSSWINDS > 15 KTS
JAN	99.0%	0.7%	0.2%
FEB	98.1%	1.6%	0.3%
MAR	98.0%	1.8%	0.2%
APR	97.6%	2.1%	0.2%
MAY	98.9%	1.0%	0.1%
JUN	98.6%	1.2%	0.2%
JUL	99.4%	0.6%	0.1%
AUG	99.6%	0.4%	0.0%
SEP	99.6%	0.3%	0.1%
OCT	99.1%	0.9%	0.0%
NOV	99.2%	0.8%	0.0%
DEC	98.9%	0.8%	0.2%

SKOPJE, MACEDONIA

MONTH	FAVORABLE CROSSWINDS < 10 KTS	MARGINAL CROSSWINDS 10-15 KTS	UNFAVORABLE CROSSWINDS > 15 KTS
JAN	97.7%	2.1%	0.2%
FEB	96.7%	2.9%	0.4%
MAR	97.3%	2.4%	0.4%
APR	96.6%	2.9%	0.5%
MAY	97.6%	2.0%	0.4%
JUN	96.3%	3.3%	0.5%
JUL	95.2%	4.0%	0.8%
AUG	96.3%	3.2%	0.5%
SEP	97.2%	2.5%	0.3%
OCT	97.4%	2.2%	0.4%
NOV	97.3%	2.4%	0.4%
DEC	97.8%	1.9%	0.2%

TUZLA, BOSNIA-HERZEGOVINA

MONTH	FAVORABLE CROSSWINDS < 10 KTS	MARGINAL CROSSWINDS 10-15 KTS	UNFAVORABLE CROSSWINDS > 15 KTS
JAN	99.6%	0.1%	0.3%
FEB	99.8%	0.2%	0.0%
MAR	99.7%	0.1%	0.1%
APR	99.3%	0.5%	0.2%
MAY	99.5%	0.3%	0.2%
JUN	99.9%	0.1%	0.0%
JUL	100.0%	0.0%	0.0%
AUG	99.7%	0.0%	0.3%
SEP	99.8%	0.0%	0.2%
OCT	99.6%	0.1%	0.3%
NOV	99.8%	0.0%	0.2%
DEC	99.8%	0.1%	0.1%

PERCENTAGE FREQUENCIES FOR CATEGORIES OF PRECIPITATION
PERIOD OF RECORD: 1973-1998

PRISTINA, YUGOSLAVIA

MONTH	FAVORABLE NO/LIGHT PRECIP	MARGINAL MODERATE PRECIP	UNFAVORABLE HEAVY PRECIP
JAN	99.0%	0.9%	0.1%
FEB	98.8%	1.0%	0.2%
MAR	99.2%	0.7%	0.1%
APR	98.9%	1.1%	0.0%
MAY	98.6%	1.4%	0.0%
JUN	98.2%	1.7%	0.0%
JUL	99.3%	0.7%	0.0%
AUG	99.0%	1.0%	0.0%
SEP	99.3%	0.6%	0.0%
OCT	99.3%	0.6%	0.1%
NOV	98.6%	1.2%	0.2%
DEC	98.7%	1.0%	0.3%

SKOPJE, MACEDONIA

MONTH	FAVORABLE NO/LIGHT PRECIP	MARGINAL MODERATE PRECIP	UNFAVORABLE HEAVY PRECIP
JAN	99.5%	0.3%	0.2%
FEB	99.0%	0.8%	0.2%
MAR	99.4%	0.6%	0.1%
APR	98.5%	1.5%	0.0%
MAY	98.6%	1.3%	0.0%
JUN	98.9%	1.1%	0.0%
JUL	99.1%	0.9%	0.0%
AUG	99.2%	0.8%	0.0%
SEP	99.1%	0.9%	0.0%
OCT	99.3%	0.7%	0.0%
NOV	99.0%	0.9%	0.1%
DEC	99.1%	0.7%	0.2%

TUZLA, BOSNIA-HERZEGOVINA

MONTH	FAVORABLE NO/LIGHT PRECIP	MARGINAL MODERATE PRECIP	UNFAVORABLE HEAVY PRECIP
JAN	98.7%	1.3%	0.0%
FEB	98.1%	1.6%	0.3%
MAR	99.1%	0.9%	0.0%
APR	98.8%	1.2%	0.0%
MAY	98.2%	1.8%	0.0%
JUN	97.6%	2.4%	0.0%
JUL	97.5%	2.5%	0.0%
AUG	98.1%	1.9%	0.0%
SEP	98.4%	1.4%	0.2%
OCT	98.3%	1.6%	0.1%
NOV	98.8%	1.2%	0.1%
DEC	98.4%	1.2%	0.4%

PERCENTAGE FREQUENCIES FOR CATEGORIES OF SKY COVER
PERIOD OF RECORD: 1973-1998

PRISTINA, YUGOSLAVIA

MONTH	FAVORABLE CLOUD COVER < 30%	MARGINAL CLOUD COVER 30-50%	UNFAVORABLE CLOUD COVER > 50%
JAN	28.1%	6.2%	65.7%
FEB	32.5%	8.4%	59.1%
MAR	34.8%	9.4%	55.9%
APR	26.9%	10.6%	62.5%
MAY	25.3%	13.9%	60.8%
JUN	35.6%	15.8%	48.6%
JUL	53.1%	14.4%	32.5%
AUG	58.6%	12.5%	28.9%
SEP	53.3%	11.7%	35.0%
OCT	43.8%	9.5%	46.7%
NOV	28.5%	7.3%	64.2%
DEC	26.9%	7.3%	65.8%

SKOPJE, MACEDONIA

MONTH	FAVORABLE CLOUD COVER < 30%	MARGINAL CLOUD COVER 30-50%	UNFAVORABLE CLOUD COVER > 50%
JAN	24.3%	6.6%	69.1%
FEB	24.3%	8.6%	67.1%
MAR	24.5%	9.5%	65.9%
APR	25.9%	13.8%	60.2%
MAY	29.0%	16.4%	54.7%
JUN	40.4%	18.1%	41.5%
JUL	53.7%	16.3%	30.0%
AUG	55.8%	14.3%	29.9%
SEP	49.7%	12.7%	37.6%
OCT	36.6%	9.6%	53.8%
NOV	24.6%	7.7%	67.7%
DEC	21.9%	6.6%	71.5%

TUZLA, BOSNIA-HERZEGOVINA

MONTH	FAVORABLE CLOUD COVER < 30%	MARGINAL CLOUD COVER 30-50%	UNFAVORABLE CLOUD COVER > 50%
JAN	20.7%	6.6%	72.7%
FEB	30.4%	7.0%	62.6%
MAR	31.9%	8.9%	59.2%
APR	23.1%	11.7%	65.2%
MAY	22.6%	13.1%	64.3%
JUN	30.0%	17.0%	53.0%
JUL	43.9%	13.5%	42.6%
AUG	39.7%	13.2%	47.1%
SEP	41.6%	11.6%	46.8%
OCT	36.2%	8.7%	55.1%
NOV	23.9%	7.1%	69.0%
DEC	20.6%	7.7%	71.7%

PERCENTAGE FREQUENCIES FOR CATEGORIES OF VISIBILITY
PERIOD OF RECORD: 1973-1998

PRISTINA, YUGOSLAVIA

MONTH	FAVORABLE VISIBILITY > 4800 M	MARGINAL VISIBILITY 3200-4800 M	UNFAVORABLE VISIBILITY < 3200 M
JAN	64.2%	17.2%	18.6%
FEB	78.0%	14.5%	7.5%
MAR	91.4%	6.9%	1.7%
APR	95.2%	4.2%	0.6%
MAY	96.0%	3.2%	0.8%
JUN	95.5%	3.4%	1.1%
JUL	95.5%	3.8%	0.7%
AUG	95.2%	4.0%	0.7%
SEP	91.6%	5.9%	2.5%
OCT	89.0%	6.8%	4.2%
NOV	75.9%	12.5%	11.5%
DEC	67.5%	16.0%	16.5%

SKOPJE, MACEDONIA

MONTH	FAVORABLE VISIBILITY > 4800 M	MARGINAL VISIBILITY 3200-4800 M	UNFAVORABLE VISIBILITY < 3200 M
JAN	57.6%	7.1%	35.3%
FEB	78.4%	5.5%	16.0%
MAR	95.3%	1.4%	3.4%
APR	98.9%	0.4%	0.6%
MAY	99.0%	0.5%	0.5%
JUN	99.6%	0.2%	0.2%
JUL	99.6%	0.2%	0.2%
AUG	99.4%	0.3%	0.3%
SEP	97.9%	1.0%	1.1%
OCT	93.6%	2.2%	4.2%
NOV	72.8%	6.3%	20.9%
DEC	56.5%	6.1%	37.4%

TUZLA, BOSNIA-HERZEGOVINA

MONTH	FAVORABLE VISIBILITY > 4800 M	MARGINAL VISIBILITY 3200-4800 M	UNFAVORABLE VISIBILITY < 3200 M
JAN	38.4%	29.1%	32.5%
FEB	44.8%	28.6%	26.6%
MAR	69.3%	17.9%	12.8%
APR	71.8%	17.5%	10.7%
MAY	76.3%	14.8%	8.9%
JUN	80.1%	13.7%	6.2%
JUL	79.4%	15.3%	5.2%
AUG	72.8%	15.8%	11.4%
SEP	64.3%	19.8%	15.9%
OCT	55.1%	23.6%	21.3%
NOV	39.9%	32.7%	27.5%
DEC	35.5%	29.7%	34.9%

PERCENTAGE FREQUENCIES FOR CATEGORIES OF WIND SPEED
PERIOD OF RECORD: 1973-1998

PRISTINA, YUGOSLAVIA

MONTH	FAVORABLE SUSTAINED WINDS < 20 KTS	MARGINAL SUSTAINED WINDS 20-30 KTS	UNFAVORABLE SUSTAINED WINDS > 30 KTS
JAN	99.6%	0.3%	0.1%
FEB	99.6%	0.4%	0.0%
MAR	99.4%	0.6%	0.0%
APR	99.8%	0.2%	0.0%
MAY	99.8%	0.2%	0.0%
JUN	99.9%	0.0%	0.1%
JUL	99.9%	0.0%	0.0%
AUG	100.0%	0.0%	0.0%
SEP	99.9%	0.0%	0.1%
OCT	99.9%	0.1%	0.0%
NOV	99.6%	0.3%	0.0%
DEC	99.6%	0.4%	0.0%

SKOPJE, MACEDONIA

MONTH	FAVORABLE SUSTAINED WINDS < 20 KTS	MARGINAL SUSTAINED WINDS 20-30 KTS	UNFAVORABLE SUSTAINED WINDS > 30 KTS
JAN	99.3%	0.7%	0.0%
FEB	98.8%	1.2%	0.0%
MAR	99.1%	0.9%	0.0%
APR	98.9%	1.1%	0.0%
MAY	99.6%	0.3%	0.0%
JUN	99.3%	0.6%	0.0%
JUL	99.1%	0.8%	0.0%
AUG	99.5%	0.5%	0.0%
SEP	99.6%	0.4%	0.0%
OCT	99.4%	0.6%	0.1%
NOV	99.3%	0.6%	0.1%
DEC	99.3%	0.5%	0.2%

TUZLA, BOSNIA-HERZEGOVINA

MONTH	FAVORABLE SUSTAINED WINDS < 20 KTS	MARGINAL SUSTAINED WINDS 20-30 KTS	UNFAVORABLE SUSTAINED WINDS > 30 KTS
JAN	99.8%	0.0%	0.2%
FEB	100.0%	0.0%	0.0%
MAR	99.7%	0.3%	0.1%
APR	99.6%	0.2%	0.2%
MAY	99.9%	0.0%	0.1%
JUN	99.8%	0.1%	0.1%
JUL	99.8%	0.1%	0.1%
AUG	99.8%	0.1%	0.1%
SEP	100.0%	0.0%	0.0%
OCT	99.8%	0.1%	0.1%
NOV	99.9%	0.1%	0.0%
DEC	99.9%	0.1%	0.0%

BIBLIOGRAPHY

Anton, Howard. Calculus with Analytic Geometry (Third Edition). New York, NY: John Wiley & Sons, 1988.

Banks, Jerry, John S. Carson, II, and Barry L. Nelson. Discrete-Event Simulation (Second Edition). Upper Saddle River, NJ: Prentice Hall, 1996.

Breshears, Brian R. "UAV Roles in the Battlespace of Tomorrow," UAVSI '96 Proceedings: 313-349 (July 1996).

Brandt. Instructor, United States Air Force Academy, Colorado Springs, CO. Telephone interview. 10 September 1998.

Department of Defense, Defense Modeling and Simulation Office. Verification, Validation, and Accreditation (VV&A) Recommended Practices Guide. http://triton.dmso.mil/dmso/docslib/mspolicy/vva/rpg/. 1996.

Jeppesen Sanderson, Inc. Private Pilot Manual. Englewood, CO: Jeppensen Sanderson, Inc., 1995.

Myers, Raymond H. and Douglas C. Montgomery. Response Surface Methodology: Process and Product Optimization Using Designed Experiments. New York, NY: John Wiley & Sons, Inc., 1995.

O'Rourke, Kevin. Dynamic Unmanned Aerial Vehicle (UAV) Routing with a Java-Encoded Reactive Tabu Search Metaheuristic. AFIT/GOA/ENS/99M. School of Engineering, Air force Institute of Technology (AU), Wright-Patterson AFB OH, March 1999.

Neter, John, Michael H. Kutner, Christopher J. Nachtsheim, and William Wasserman. Applied Linear Statistical Models (Fourth Edition). Chicago, IL: Irwin, 1996.

Ryan, Joel L, T. Glenn Bailey, James T. Moore, and William B. Carlton. "Unmanned Aerial Vehicle (UAV) Route Selection Using Reactive Tabu Search," to appear in Military Operations Research.

Sall, John and Ann Lehman, SAS Institute, Inc. JMP Start Statistics A Guide to Statistics and Data Analysis Using JMP and JMP IN® Software. New York, NY: Duxbury Press, 1996.

Sisson, Mark R. Applying Tabu Heuristic to Wind Influenced, Minimum Risk and Maximum Expected Coverage Routes. AFIT/GOR/ENS/97M. School of Engineering, Air Force Institute of Technology (AU), Wright-Patterson AFB OH, February 1997.

Stoneman, James G. Operational Analysis of the Sustainability of a Mobile Military Platform. AD-A354 297/XAF. Naval Post Graduate School, Monterey, CA, 1998.

Theisen, Paul. Unmanned Aerial Vehicle Battlelab, 1003 Nomad Way, Eglin AFB, FL. Telephone interview, 3 August 1998.

United States Air Force, Air Combat Command. Kenney Battlelab Initiative: Active SEAD. Draft 1998a.

United States Air Force, Air Combat Command. Concept of Operations for Endurance Unmanned Aerial Vehicles. (Version 3) 1998b.

United States Army Materiel Command. "Operations Research and Systems Analysis Awards." Award Citations, n. pag. http://amsaa-www.arl.mil/cp16/awards.htm. 14 July 1998.

Wackerly, Dennis D., William Mendenhall III, and Richard L. Scheaffer. Mathematical Statistics with Applications (Fifth Edition). New York, NY: Duxbury Press, 1996.

Vita

Jennifer G. Walston was born in Topeka, Kansas, on 12 September 1972, the daughter of Russell E. Wells, and Jillana J. Wells. In June 1991 she graduated from Crafton Hills College, in Yucaipa, California, earning an Associate of Science in Physics. In June 1994 she graduated from California Polytechnic State University, at San Luis Obispo, earning a Bachelor of Science in Aeronautical Engineering. After graduation, she accepted a commission in the United States Air Force. While serving on active duty at the Air Force Operational Test and Evaluation Center, she became a fully qualified Missile Maintenance Officer and Senior Space Systems Suitability Manager. She married Bradley W. Walston on 28 December 1996. She entered the Graduate School of Engineering, Air Force Institute of Technology August of 1997.

Permanent Address:

6606 Holford Ln.
Springfield Virginia
22152-2908

REPORT DOCUMENTATION PAGE

Form Approved
OMB No. 0704-0188

1. AGENCY USE ONLY *(Leave blank)*	2. REPORT DATE	3. REPORT TYPE AND DATES COVERED
	March 1999	Master's Thesis

4. TITLE AND SUBTITLE
UNMANNED AERIAL VEHICLE MISSION LEVEL SIMULATION

5. FUNDING NUMBERS

6. AUTHOR(S)
Jennifer G. Walston, Captain, USAF

7. PERFORMING ORGANIZATION NAME(S) AND ADDRESS(ES)
Air Force Institute of Technology
2950 P Street
WPAFB OH 45433-7765

8. PERFORMING ORGANIZATION REPORT NUMBER
AFIT/GOR/ENS/99M-17

9. SPONSORING/MONITORING AGENCY NAME(S) AND ADDRESS(ES)
Lt Col Mark O'Hair
Unmanned Aerial Vehicle Battlelab (UAVB)
1003 Nomad Way, Suite 107
Eglin AFB FL 32542-6867

10. SPONSORING/MONITORING AGENCY REPORT NUMBER

11. SUPPLEMENTARY NOTES

12a. DISTRIBUTION AVAILABILITY STATEMENT
Approved for public release; distribution unlimited

12b. DISTRIBUTION CODE

13. ABSTRACT *(Maximum 200 words)*

We develop an object-oriented simulation that models the surveillance and Active Suppression of Enemy Air Defense (SEAD) missions of the Unmanned Aerial Vehicle (UAV) RQ-1A Predator. The simulation, written in Java using the Silk simulation package, interfaces with a Reactive Tabu Search routing algorithm to provide optimal UAV routes. The routing algorithm is called by the simulation to account for changes in weather conditions and to provide a means of dynamically retasking the UAV. The simulation and analysis support a UAV Battlelab initiative to test the operational effects of proposed changes in Predator performance and UAV capability to perform in an Active SEAD mission. Analysis efforts examine the effect of speed, endurance, and weather susceptibility on UAV operational effectiveness and the effects of radar cross section, threat density, and threat lethality on UAV Active SEAD mission performance.

14. SUBJECT TERMS	15. NUMBER OF PAGES
Discrete Event Simulation, Object-Oriented, Reactive Tabu Search, Unmanned Aerial Vehicle (UAV), RQ-1A Predator, Suppression of Enemy Air Defense (SEAD)	72
	16. PRICE CODE

17. SECURITY CLASSIFICATION OF REPORT	18. SECURITY CLASSIFICATION OF THIS PAGE	19. SECURITY CLASSIFICATION OF ABSTRACT	20. LIMITATION OF ABSTRACT
Unclassified	Unclassified	Unclassified	UL